

Title: Distinct subdivisions of human medial parietal cortex support recollection of people and places

Authors: Edward H Silson^{1*}, Adam Steel^{1,2*}, Alexis Kidder¹, Adrian W Gilmore¹, & Chris I Baker¹

Affiliations:

1. Laboratory of Brain & Cognition, National Institute of Mental Health, Bethesda, MD, USA.
2. Wellcome Centre for Integrative Neuroimaging, FMRIB, Nuffield Department of Clinical Neurosciences, University of Oxford, Oxford, OX3 9DU, UK.

Corresponding author: ed.silson@nih.gov

* equal contributions

Abstract

Human medial parietal cortex (MPC) is implicated in multiple cognitive processes including memory recall, visual scene processing and navigation, and is a core component of the default mode network. Here, we demonstrate distinct subdivisions of MPC that are selectively recruited during memory recall of either specific people or places. First, distinct regions of MPC exhibited differential functional connectivity with medial and lateral regions of ventral temporal cortex (VTC). Second, these same medial regions showed selective, but negative, responses to the visual presentation of different stimulus categories, with clear preferences for scenes and faces. Finally, and most critically, these regions were differentially recruited during memory recall of either people or places with a strong familiarity advantage. Taken together, these data suggest that the organizing principle defining the medial-lateral axis of VTC is reflected in MPC, but in the context of memory recall.

Introduction

Human medial parietal cortex (MPC), a core component of the default mode network (DMN) (Andrews-Hanna et al. 2010), comprises a relatively large expanse of cortex, spanning the parieto-occipital sulcus to the splenium of the corpus collosum anteriorly and dorsally to include the precuneus and both the ventral and dorsal portions of the posterior cingulate cortex (Bzdok et al. 2015). MPC is associated with a diverse set of cognitive functions, including (but not restricted to) memory recall (Vilberg and Rugg 2008; Wagner et al. 2005; Gilmore et al. 2015; Kim 2013) visual scene perception (Epstein et al. 2007; Silson et al. 2016; Baldassano et al. 2013), scene construction (Hassabis et al. 2007), processing of spatial and other contextual associations (Bar and Aminoff 2003), navigation (Epstein 2008), future thinking (Benoit et al. 2015; Szpunar et al. 2007; Gilmore et al. 2016), and mental orientation (Peer et al. 2015). Given such diverse recruitment of MPC across cognitive domains historically considered largely independent (e.g. visual processing, memory), the absence of a clear consensus with regard to the function and overarching organization of MPC is perhaps unsurprising (Gilmore et al. 201; Chrastil 2018).

Network analyses using resting-state-functional-connectivity (RSFC) have identified either a single DMN “hub” region (Buckner et al. 2008) or multiple networks (Power et al. 2014; Braga and Buckner 2017; Gilmore et al. 2018) that are often described as DMN subnetworks (Andrews-Hanna et al. 2010; Yeo et al. 2011; Doucet et al. 2011). Task-based analyses also suggest a fractionation beyond a single region (Andrews-Hanna et al. 2010; Peer et al. 2015; Chrastil 2018), with, for example, evidence that the

ventral and dorsal portions of posterior cingulate cortex interact differently with the rest of DMN during cognitive control (Leech et al. 2011). Further, recent work has reframed MPC (and the DMN) in terms of large-scale cortical gradients (Margulies et al. 2016), conceptualizing MPC as the most abstract extension of the ventral visual pathway (Murphy et al. 2018; 2019). Beyond MPC's link with the DMN, others have described divisions of MPC along both the posterior-anterior and ventral-dorsal axes in terms of cytoarchitecture (Vogt, 2009), structural connectivity (Parvizi et al. 2006), RSFC (Margulies et al. 2009; Vidaurre et al. 2018; Bzdok et al. 2015), and electrocorticography (Foster et al. 2012; Daitch & Parvizi, 2018).

The question of the underlying functional organization of MPC is clearly complicated and could potentially benefit from a simple and more unified perspective. A promising lead on one such organization has come from recent work demonstrating a strong functional link between anterior ventral temporal cortex (VTC) and MPC (Baldassano et al. 2013; 2016; Silson et al. 2016). Specifically, a small region of MPC directly anterior of (visually) scene-selective medial place area (MPA) (Silson et al. 2016) showed strong functional connectivity with anterior portions of scene-selective parahippocampal place area (Epstein 2008) (aPPA), located in medial VTC. This connectivity-defined region overlaps with regions of MPC engaged during memory recall (Silson et al., 2019), suggesting that the ventral/posterior aspect of MPC may contain distinct areas biased toward scene processing for vision and memory, respectively.

What else might we learn from examining potential links between MPA and VTC? Whilst the previous functional link between MPC and VTC was based upon parcellating PPA along its posterior-anterior axis, the functional organization of VTC varies more dramatically along the orthogonal medial-lateral axis. Indeed, multiple functional dimensions are thought to be represented along this axis, including category preference (Kanwisher et al. 1997; Deen et al. 2017) (e.g. scenes, objects, tools and faces), eccentricity (Levy et al. 2001; Arcaro and Livingstone 2017) (e.g. peripheral, foveal), animacy (Konkle and Caramazza 2013), and even real-world size (Konkle and Oliva 2012). Further, the mid-fusiform sulcus (MFS) (Weiner et al. 2014) has been identified as an anatomical landmark marking a transition point within each dimension (e.g. scene-selectivity medial of the MFS, face-selectivity lateral of the MFS). These robust functional differences across the medial-lateral axis of VTC—and their well-characterized, category-specific nature—may provide an effective perspective from which to investigate the organizational structure of MPC.

To investigate whether the functional organization of MPC reflects that of VTC, we conducted three independent fMRI experiments. First, we found that distinct subdivisions of MPC have preferential functional connectivity to anterior portions of medial and lateral VTC, respectively. Second, these MPC subdivisions showed differential evoked responses to the presentation of different visual categories, with clear evidence for scene and face preferences. Third, and most critically, these subdivisions were selectively recruited during memory recall of either specific places (i.e. scenes) or specific people (i.e. faces). Finally, an independent whole-brain analysis

of memory recall effects revealed an even finer division within MPC, with four identifiable regions showing an alternating (place/people) pattern of selective recruitment during memory recall.

Taken together, these findings provide converging evidence for a reflection of the functional organization of VTC in MPC. This organization was evident at rest, in response to visual stimulation, and most strikingly, during memory recall. The alternating pattern of responses throughout MPC provides a framework for understanding the broader functional organization of MPC and may tie together many of the disparate observations reported across the literature. Collectively, these data support the notion that the functional organization defining the medial-lateral axis of VTC is reflected along the ventral/posterior-dorsal/anterior axis MPC, but in the context of memory retrieval.

Results

Subdivisions of MPC show preferential functional connectivity with medial and lateral portions of VTC

To determine whether the functional organization along the medial-lateral axis of VTC is reflected in MPC, we first utilized resting-state functional connectivity data (n=65). Six regions of interest (ROIs) were defined anatomically in each hemisphere that divided VTC along both the posterior-anterior and medial-lateral axes with respect to the MFS (Weiner et al. 2014), allowing us to characterize the connectivity profile between VTC and MPC more precisely (**Fig. 1a**). A winner-take-all analysis (**see Methods**) revealed a

ventral-posterior MPC region (referred to as MPC ventral, MPCv) that showed strongest connectivity with the anterior medial ROI and an adjacent dorsal-anterior region (referred to as MPC dorsal, MPCd) that showed strongest connectivity to the anterior lateral ROI (**Fig. 1b**). Such a pattern of connectivity suggests a reflection of the functional organization defining the medial-lateral axis of VTC along the posterior/ventral-anterior/dorsal axis of MPC.

Subdivisions of MPC show differential responses to visually presented categories

Having identified distinct subdivisions of MPC based on differential functional connectivity with anterior portions of medial and lateral VTC, we next sought to determine whether these subdivisions would respond differentially to the visual presentation of different stimulus categories (Scenes, Faces, Buildings, Bodies, Objects and Scrambled Objects) (**see Methods**). Differentiation on the basis of stimulus category would be reminiscent of the category-preference changes along the medial-lateral axis of VTC.

In a second independent group of participants (n=29), we calculated the mean response to each category (given as the *t*-value versus baseline) in both ROIs and hemispheres separately. Unlike category-selective regions of VTC (e.g. PPA, Fusiform Face Area, FFA), which typically exhibit positive responses to the presentation of visual stimuli, we observed negative response magnitudes to all categories within both MPC subdivisions. Despite this general tendency for negative magnitudes, responses also appeared to differentiate on the basis of category, with scenes evoking the strongest response (i.e.

least negative) in MPCv and faces evoking the strongest response in MPCd of both hemispheres (**Fig. 2**).

To explore these effects further, mean response magnitudes for each category were subjected to a one-way repeated measures Analysis of Variance (ANOVA) with Category (6 levels) as a within-participant factor. MPCv exhibited a significant main effect of Category in both the left ($F_{(5, 140)}=71.38$, $p<0.0001$, partial $\eta^2=0.72$) and right ($F_{(5, 140)}=49.46$, $p<0.0001$, partial $\eta^2=0.64$) hemispheres. Consistent with the stronger functional connectivity with medial VTC, the response to scenes was significantly different from other stimulus categories in both hemispheres ($t > 5.34$, $p<0.001$, in all cases, Bonferroni corrected) (**Fig. 2a**).

MPCd also exhibited a significant effect of Category within both left ($F_{(5, 140)}=19.28$, $p<0.0001$, partial $\eta^2=0.48$) and right ($F_{(5, 140)}=12.66$, $p<0.0001$, partial $\eta^2=0.31$) hemispheres. However, in this case the response to faces was only significantly different from Buildings and Scrambled Objects in the left hemisphere ($t > 3.86$, $p<0.001$, Bonferroni corrected; $p>0.05$, in all other cases), whereas the response to faces was significantly different from all categories except Objects ($p>0.05$) in the right hemisphere ($t > 3.54$, $p<0.001$, Bonferroni corrected) (**Fig. 2b**). Collectively these results demonstrate a preference for scenes and faces within MPCv and MPCd, respectively. The overall pattern of negative responses evoked by visual stimuli is consistent with the widely-reported negative responses within MPC (and the broader DMN) when orienting to external stimuli²⁷. However, motivated by the apparent scene

and face preference within these regions and the fact that MPC is typically engaged positively during introspective tasks such as scene-construction from memory and mental imagery, we hypothesized that these MPC subdivisions would become differentially recruited during memory recall of either specific places (MPCv) or specific people (MPCd), respectively.

Subdivisions of MPC differentially recruited during memory recall of specific places or specific people

To investigate the hypothesis that MPCv/MPCd would be differentially recruited during memory recall of specific places and people, respectively, we conducted a memory recall experiment in a third independent group of participants (n=24). Participants performed six runs of a memory recall task, in which they were cued to recall from memory either specific places or specific people. Here, a simple 2 x 2 design was employed with two categories (Places, People) and two levels of familiarity (Famous, Personal) (**Fig. 3a**). Such a design allowed us to test the predictions that MPCv/MPCd would be selectively recruited during recall of specific places and people, respectively, whilst the addition of personally relevant stimuli provided a means to assess whether such category-selective recruitment was dependent on the richness of internal representations. In order to test this hypothesis, we looked in each region for the effects of category, familiarity and their potential interaction.

Subdivisions within MPC showed strikingly different response profiles during memory recall (derived by averaging the evoked responses across all trials per condition). Within MPCv, responses were maximally positive (relative to baseline) for the recall of

personally familiar places, whereas responses during recall of famous people were maximally negative (**Fig. 3b**). In contrast, responses within MPCd were maximally positive for the recall of personally familiar people and maximally negative during recall of famous places (**Fig. 3c**). To quantify these responses, we calculated the mean contrast response (given by the t -value versus baseline) within each ROI to all conditions from the GLM analysis (**See Methods**). These responses were then subjected to a three-way repeated measures ANOVA for each ROI separately, with Category (People, Places), Familiarity (Famous, Personal) and Hemisphere (Left, Right) as within-participant factors. **MPCv selectively recruited during memory recall of specific places**

Within MPCv, the main effects of Category ($F_{(1, 23)}=75.40$ $p=1.02^{-8}$, partial $\eta^2=0.76$), Familiarity ($F_{(1, 23)}=128.61$ $p=6.78^{-11}$, partial $\eta^2=0.85$) and Hemisphere ($F_{(1, 23)}=4.92$ $p=0.03$, partial $\eta^2=0.17$) were significant, reflecting on average greater responses for the recall of places over people, personal over famous stimuli and in the right compared to left hemisphere, respectively. However, these main effects were qualified by a significant three-way interaction (Category by Familiarity by Hemisphere: $F_{(1, 23)}=7.19$ $p=0.01$, partial $\eta^2=0.24$). This interaction reflects a larger familiarity difference (Personal > Famous) between categories (Place > People), in the right over left hemisphere. Further, we performed separate two two-way ANOVAs in each hemisphere separately with Category and Familiarity as factors. In both hemispheres, the Category by Familiarity interaction was significant (Left: $F_{(1, 23)}=31.19$, $p=0.00001$, partial $\eta^2=0.56$; Right: $F_{(1, 23)}=49.51$, $p=3.59^{-7}$, partial $\eta^2=0.68$), reflecting a larger familiarity difference for the recall of places over people in both hemispheres (**Fig. 4a**).

MPCd selectively recruited during memory recall of specific people

Within MPCd, the main effects of Category ($F_{(1, 23)}=47.53$ $p=4.98^{-7}$, partial $\eta^2=0.67$), Familiarity ($F_{(1, 23)}=82.33$ $p=4.62^{-9}$, partial $\eta^2=0.78$) and Hemisphere ($F_{(1, 23)}=10.70$ $p=0.003$, partial $\eta^2=0.32$) were again significant, reflecting on average greater responses for the recall of people over places, personal over famous stimuli and in the right compared to left hemisphere, respectively. Whilst, we did not observe a significant three-way interaction, several significant two-way interactions were observed. Importantly, the Category by Familiarity interaction ($F_{(1, 23)}=7.89$ $p=0.01$, partial $\eta^2=0.25$), was significant, which reflects a larger familiarity difference for the recall of people over places with no clear difference between hemispheres (**Fig. 4b**). (see **Supplementary File 1b for full statistical breakdown**).

Consistent topography of memory recall effects within MPC

Both MPC subdivisions showed differential recall effects for places and people, respectively, coupled with an overall familiarity advantage. The topography of this differential recruitment during recall was strikingly consistent across individuals. Indeed, throughout MPC comparisons of the peak locations for the recall of personal places and personal people demonstrates a consistent shift along the ventral/posterior–dorsal/anterior axis. Across all participants and hemispheres, the peak response during recall of personal people was always anterior and dorsal to the peak response during recall of personal places (**Fig. 5**).

Alternating pattern of place and people memory recall throughout MPC

Having established that subdivisions of MPC are differentially recruited during memory recall, we next sought to determine whether areas outside of these initial ROIs showed similar effects. Accordingly, we performed a whole-brain Linear-Mixed-Effects (LME) modelling analysis to look for regions of the brain displaying main effects of Category (Places, People), Familiarity (Famous, Personal) and their interaction (**see Methods**). At the whole-brain level, we did not observe any regions showing a significant interaction (at the selected statistical threshold), although significant responses to both main effects were present. The main effect of Category (collapsed across familiarity) revealed a complex pattern of differential recruitment throughout the brain. Most strikingly, along the ventral/posterior-dorsal/anterior axis of MPC, we observed an alternating pattern of memory recall: four adjacent subdivisions that alternated between being selectively recruited by the recall of places, then people, then places and finally people (**Fig. 6a**). Notably, the first two subdivisions (referred to here as ROIs 1 & 2) were largely equivalent to the connectivity-defined MPCv and MPCd (**see Supplementary Material for spatial overlap**). Thus, this analysis not only confirmed the differential recruitment during memory recall of MPCv and MPCd, but also, revealed two anterior subdivisions within bilateral MPC that showed similar patterns of selective recruitment (ROIs 3 & 4). Strong memory recall for places was also present in aPPA in both hemispheres (**Fig. 6a**). In contrast to the alternating pattern of place and people recall, the effect of familiarity (collapsed across category) manifested as an advantage for the recall of personally familiar over famous stimuli, irrespective of category within a relatively large swath of MPC (**Fig. 6b**).

To quantify the selective recruitment within each of these four MPC subdivisions in an independent manner, we implemented a split-half analysis. First, in each participant, we divided the six memory runs into odd and even datasets (3 runs each). Next, we performed the same LME analysis as above in each dataset separately (**see Methods**). Between the odd and even splits, the topography and magnitude of the effect of category was robust and highly correlated across splits and hemispheres, respectively (left hemisphere: $r = .81$, $R^2 = 0.65$; right hemisphere: $r = .84$, $R^2 = 0.71$) (**Fig. 7a**). In order to determine estimates of effect size, we defined each MPC subdivision in one half the data (e.g. Odd) and sampled the responses to all conditions from the other half (e.g. Even). This process was then reversed, and the average computed. We observed a consistent and alternating pattern of selective recruitment throughout MPC. Recall of specific places selectively recruited ROIs 1 and 3, whereas recall of specific people selectively recruited ROIs 2 and 4. Consistent with our initial analyses, all four MPC subdivisions exhibited a familiarity advantage, which manifested as a selective enhancement in response for personally familiar items (Places = ROIs 1 and 3, People = ROIs, 2 and 4) (**see Supplementary File 1c-1f for full statistical breakdown**).

Memory recall effects beyond MPC

Significant effects of place and people recall were also evident throughout the brain. In particular, the posterior angular gyrus, inferior temporal sulcus, and superior frontal regions were recruited during place recall, whereas the recall of people recruited the insula and anterior temporal regions, particularly in the right hemisphere (**Figure 6-figure supplement 1**). Advantages for the recall of personally familiar stimuli were

present within anterior cingulate cortex and insula in both hemispheres (**Fig. 6b**), as well as regions on the lateral surface, including superior-frontal, the superior-temporal sulcus, and angular gyrus/caudal inferior parietal lobule (**Figure 6-figure supplement 1**). In contrast, recall effects associated with famous over familiar stimuli were sparse and non-significant.

Memory recall effects were also observed within functionally-defined scene- and face-selective regions of VTC (i.e. PPA, FFA). Both regions were recruited during recall of items from their preferred category (i.e. greater response to place-specific memory in PPA, greater response to people-specific memory in FFA), although the magnitude of these memory effects were markedly weaker than within MPC (**Figure 6-figure supplement 2** and **see Supplementary File 1g for full statistical breakdown**).

In addition to cortical ROIs, significant memory recall effects were also present in the hippocampus and amygdala bilaterally. The hippocampus showed an effect of category, with larger responses during recall of places over people, whilst also showing a strong familiarity advantage with larger responses for personally familiar over famous stimuli (**Figure 6-figure supplement 3**). In contrast, the amygdala showed only an effect of category, with larger responses during recall of people irrespective of the level of familiarity (**Figure 6-figure supplement 3; see Supplementary File 1h for full statistical breakdown**).

Discussion

Across three independent fMRI experiments, we demonstrate two major subdivisions of MPC that exhibit i) differential functional connectivity to medial and lateral portions of anterior VTC, ii) show negative BOLD responses during visual perception with clear preferences for scenes and faces and iii) are differentially recruited during memory recall for either specific places or specific people. Further, at the whole-brain level we identify a second pair of anterior regions, which exhibit the same selective recruitment during memory recall for places and people, revealing a total of four subdivisions within MPC. Taken together, these findings provide converging evidence that the functional organization defining the medial-lateral axis of VTC is reflected along the ventral/posterior-dorsal/anterior axis of MPC, but in the context of memory recall.

The functional organization of medial parietal cortex

The selective recruitment of MPC during recall of places or people is consistent with a diverse literature linking MPC with multiple memory processes (Vilberg and Rugg 2008; Wagner et al. 2005; Gilmore et al. 2015; Kim 2013). Unlike previous neuropsychological work (Valenstein et al. 1987; Arnott et al. 2008; Gainotti et al. 1998), which lacked the spatial specificity to examine the heterogeneity of MPC or neuroimaging work that has associated MPC divisions with broad domain-level processes (Wagner et al. 2008; Andrews-Hanna et al. 2010), we provide evidence for a set of functionally dissociable sub regions along the ventral/posterior-dorsal/anterior axis of MPC that appear selective for places and people, reminiscent of category-selective areas along the medial-lateral axis of VTC.

Initially, we focused on two MPC subdivisions, defined on the basis of preferential functional connectivity to medial and lateral portions of anterior VTC, respectively. These subdivisions exhibited different (albeit negative) responses to visually presented categories and were differentially recruited during memory recall. During the recall of specific places, MPCv showed strong positive evoked responses, which contrasted with negative evoked responses during the recall of specific people. In contrast, MPCd showed largely the opposite pattern - large positive evoked responses during recall of personally familiar people, but not during the recall of either famous people or places. These data show a clear division between ventral/posterior and dorsal/anterior portions of MPC based on the content of the recalled memory. This division is broadly consistent with prior anatomical (Vogt, 2009; Parvizi et al. 2006) and functional imaging (Marguiles et al. 2009; Vidaurre et al. 2018; Foster et al. 2012; Marguiles et al. 2016; Peer et al. 2015) work that also identified divisions within MPC along this axis, but did not do so on the basis of recalled content.

The cortical locations of MPCv/MPCd are consistent with previous observations of memory related activity (Andrews-Hanna et al., 2010; Peer et al. 2015; Gilmore et al. 2018; Kuhl & Chun, 2014; Chen et al. 2017). Indeed, the locations of MPCv/MPCd are qualitatively similar to regions recruited when participant's mentally oriented by either making egocentric distance judgments between two places (i.e. which location is physically closest to them), or between two people (i.e. which of two people are personally closer to them), respectively (Peer et al. 2015). Although such a distance judgement undoubtedly requires recalling specific information, our findings suggest that

an explicit distance task is not required to functionally isolate MPCv and MPCd. In the current study, participants were not asked to make social and spatial distance judgments, but merely to recall from memory either specific people or places. This, we believe, provides strong evidence for the role that MPCv/MPCd play in our ability to recall specific features from memory—and seemingly in a manner that recapitulates VTC organization.

Importantly, we also identify a second pair of anterior regions along the same ventral/posterior-dorsal/anterior axis, that fall anterior of the ‘place’ and ‘people’ regions reported by Peer et al (2015), revealing a total of four subdivisions selectively recruited during memory recall for people or places in an alternating pattern. One intriguing feature of this anterior pair of regions was that the pattern of selective recruitment remained despite an overall reduction in the magnitude of responses to recalled stimuli, as compared to MPCv/MPCd. The location of this anterior pair appears qualitatively similar to the ‘time’ region identified by Peer et al (2015). It is possible that the posterior and anterior pairs we identified play complementary and yet different roles in representing information about people and places. Elucidating any potential differences between these pairs of regions and how they may relate to the representations of time reported by Peer et al (2015) are key goals for future work.

A major contribution of the current work is the demonstration that the functional organization defining the medial-lateral axis of VTC is reflected along the ventral/posterior-dorsal/anterior axis of MPC. The present work informs other recent

parcellations of MPC (Chrastil 2018; Power et al. 2014; Braga and Buckner 2017; Yeo et al. 2011). For example, a recent meta-analysis attempted to divide a ventral portion of MPC (referred to as retrosplenial complex) on the basis of different fMRI task activations (Chrastil 2018). Although the majority of MPC was found to be recruited during memory tasks, a ventral/posterior region was more likely to be recruited during scene and navigation-related tasks, whilst more dorsal/anterior portions were more likely to be involved in theory-of-mind and social/emotional tasks. Similarly, a recent report (Andrews-Hanna et al. 2010) separated social regions of MPC (i.e. those engaged with theory-of-mind tasks) from those involved with constructive memory or the formation of contextual associations (Hassabis et al. 2007; Bar and Aminoff, 2003). These divisions align well with the differential memory recall effects reported here. The dorsal and ventral divisions also align well with recent studies that have attempted to map social network representations (Parkinson et al. 2017) and representations of familiar scenes (Sugiura et al. 2005), respectively. Our results provide a framework for understanding these previously-reported mnemonic effects by highlighting the apparent organizational link between the ventral/posterior-dorsal/anterior axis of MPC and the medial-lateral axis of VTC. Perhaps more importantly, these robust effects were evoked by the relatively simple task of recalling items that were cued by word stimuli only (or even merely perceiving presented stimuli), as opposed to performing more complex contextual association (Hassabis et al. 2007), navigation (Chrastil 2018), social judgment (Parkinson et al. 2017), or mental orientation tasks (Peer et al. 2015). Such strong recruitment of MPC through a simple paradigm is consistent with recent work showing that MPC (and the larger DMN) plays a role in simple spatial judgments of

shapes and objects, particularly when made from memory (Konishi et al. 2015; Murphy et al. 2018; 2019). Consequently, these simple paradigms pave the way for future research to potentially address functional heterogeneity in MPC using tasks that target specific cognitive processes.

Relating MPC to large-scale cortical networks

The role of MPC is often considered in the context of the DMN (Andrews-Hanna et al. 2010). Although initially conceived as a singular entity (Raichle et al. 2001), the DMN has more recently been divided into two (Shirer et al. 2012) or three (Andrews-Hanna et al. 2010) subnetworks. In the “three network” framework, much of MPC and ventral medial prefrontal cortex act as a “core” that flexibly integrates information between the “dorsal” and “ventral” subnetworks (Andrews-Hanna et al. 2010). Our results challenge this ‘core’ conceptualization by suggesting that MPC is fractionated along the same lines as these subnetworks: the dorsal component of the DMN, which overlapped regions recruited during people memory, is associated with social/semantic processing (Andrews-Hanna et al. 2010) (**Fig. 8a**), while, the ventral component, which is often referred to as a ‘scene construction’ or ‘contextual association’ (Hassabis et al. 2007; Bar and Aminoff 2003) network overlaps with regions recruited during place memory (**Fig. 8b**).

In the “two network” framework (Shirer et al. 2012) the DMN is comprised of dorsal and ventral subnetworks without a clear integrative ‘core’. This framework is also consistent with recent work using highly-sampled participants to identify two parallel and

interdigitated networks spanning cortex (Braga and Buckner 2017). These two functional networks—both of which appeared to overlap with the canonical DMN—could be differentiated through functional connectivity, given sufficient data, but stopped short of describing their specific functional organization. Our data provide a possible functional account of these networks by anchoring them to differential recruitment based on the content of perceived images as well as recalled memories, and moreover, demonstrate that such an interdigitated pattern of regions can be identified at the group-level given appropriate tasks.

The MPC regions we report also appear to overlap with the recently proposed “posterior medial” (PM) memory system and the effects we observe are broadly consistent with the notion that the PM system is involved in recollecting episodic details, constructive uses of memory, and social cognition (Ranganath and Ritchey 2012). However, the present work suggests a differentiation within the PM system based on the recall of places and people, which was not discussed originally, suggesting that MPC’s role in memory recall does not fit neatly into a simple “binary systems” model. More recently, a parietal memory network (PMN) (Gilmore et al. 2015, McDermott et al. 2017) has been identified, which includes regions within both lateral parietal cortex and MPC that are thought to be distinct from those within the DMN/PM (Yang et al. 2013; Yang et al. 2019; Gilmore et al. 2019a; Gilmore et al. 2019b) system. The memory effects we report overlap with DMN regions and appear close to, but separate from, those within the PMN (i.e., do not extend to mid-cingulate cortex or posterior aspects of the precuneus). This

450 adjacency reinforces the conceptual separation of processes associated with the PMN
451 and the DMN/PM system, respectively.

452

Functional correspondence between VTC and MPC

Multiple interrelated functional organizations are thought to be represented along the medial-lateral axis of VTC (Kanwisher et al. 1997; Deen et al. 2017; Levy et al. 2001; Arcaro and Livingstone 2017; Konkle and Caramazza 2013). How the current data fit in the context of these organizations thus requires careful consideration.

Category-selectivity is one organizing principle thought to define the medial-lateral axis of VTC. Even at early stages of cortical development (Deen et al. 2017; Arcaro and Livingstone 2017), category-selective regions appear in stereotypical locations across individuals. This consistency across individuals and developmental time-frames supports the notion that categories are represented within discrete regions of VTC. The pattern of functional-connectivity, perceptual and memory recall effects we report are consistent with the presence of this motif within MPC. However, other functional dimensions are also thought to be represented along the medial-lateral axis of VTC, and the extent to which they interact and relate to one-another, and in-turn relate to the organization of MPC, is an open question (Arcaro and Livingstone 2017; Livingstone et al. 2019).

For example, eccentricity also varies systematically along the medial-lateral axis of VTC (Levy et al. 2001). Indeed, these eccentricity representations are so highly correlated with category preference (e.g. PPA is peripherally biased, whereas FFA is foveally biased) that eccentricity has been suggested to form a prototypical organization onto which such selectivity later develops with visual experience (Silson et al. 2015; Arcaro

and Livingstone 2017). It may be that the selective recruitment we observe in MPC during memory recall arises in a similar manner: That is, it is possible that the development of categorical-preference in VTC during perception drives the development of categorical-preference in MPC for memory. Such a proposition is compatible with recent work focusing on large-scale cortical gradients that conceptualized the DMN, including MPC, as an abstract extension of VTC (Margulies et al. 2016), although in the current study we observed effects that appeared to follow a distinct regional—rather than gradient-like—organization. Alternatively, it is possible that the manner in which mnemonic representations of places and people are encoded and retrieved in MPC, differ in a way reminiscent of how the visual perception of places and people in VTC differ in terms of peripheral/foveal stimulation (**Figure 7-figure supplement 1**). The correspondence between MPC organization and the multiple dimensions thought to be represented across VTC, are key questions for future research. Importantly, these accounts are consistent with theories that suggest the organization of category representations in the brain are determined by the underlying structural (i.e. anatomical) and functional (e.g. perceptual) template (Martin 2016).

Nature of responses within MPC during perception

The responses of MPCv/MPCd during perception share similarities with VTC but differ in important ways. For instance, responses in VTC during perception are characterized by larger evoked positive responses to stimuli of the preferred category (Silson et al. 2016). In contrast, perceptual responses within MPCv/MPCd were best characterized by negative evoked responses that were attenuated, although not extinguished, by

category-preference. Despite appearing to share category representations, there was no clear relationship between the positively and negatively evoked responses between the VTC regions and their paired MPC region (e.g. anterior medial VTC – MPCv), at least at the across participant level. Although the relationship between negative BOLD-signal changes and the underlying neural activity is an area of ongoing research (Shumel et al. 2002; 2006) and has been associated with inhibition in visual cortex (Smith et al. 2004), this response is consistent with the widely-observed ‘task-negative’ activation of the larger DMN and the MPC component of it (Andrews-Hanna et al. 2010). The current study did not compare directly the responses to perceived and subsequently recalled stimuli. It is possible that the degree of attenuation of the negative response during perception is related to the degree of recruitment during recall in MPCv/MPCd (for related discussion, see Daselaar et al. 2004; 2009).

Conclusion

In this study we identified a consistent differentiation of regions within MPC, providing a new framework for understanding and investigating the functional organization of MPC and its role in memory retrieval. This differentiation was present at rest, in response to visually presented stimuli and finally through memory recall. Such division of MPC is consistent with previous anatomical (Vogt 2009) and functional (Marguiles et al. 2016; Peer et al. 2015; Foster et al. 2012, Andrews-Hanna et al. 2014; Leech et al. 2011) distinctions but suggests that these divisions can be seen on the basis of recalled content. These data provide converging evidence that the functional organization

defining the medial-lateral axis of VTC is reflected along the ventral/posterior-dorsal/anterior axis of MPC, but in the context of memory recall.

Figure legends:

Fig. 1: Resting-state functional connectivity seed regions and connectivity-defined regions of interest. **a.** A ventral view of the left hemisphere is shown with the ventral temporal cortex (VTC) highlighted with the dashed-black box, which is enlarged inset. Overlaid onto this enlarged surface are the six anatomically defined regions of interest that divide VTC along both the posterior-anterior and medial-lateral axes with respect to the mid-fusiform sulcus (MFS). The occipitotemporal sulcus (OTC) and collateral sulcus (CoS) are also labeled for reference. **b.** A medial view of the left hemisphere is shown with medial parietal cortex (MPC) highlighted by the dashed-black box, which is enlarged inset. Overlaid onto this enlarged surface is the result of the winner-take-all functional connectivity analysis. Colors on the brain correspond to the color of the anatomical ROIs in **a**. Within MPC, two separate regions are clearly visible. The ventral/posterior region (red-outline) is preferentially connected to anterior medial portions of VTC, whereas the dorsal/anterior region (blue-outline) is preferentially connected to anterior lateral portions of VTC. We define these resting-state ROIs as MPC ventral (MPCv) and MPC dorsal (MPCd), respectively.

Fig. 2: Negative responses in MPC to visually presented stimuli. **a.** Bars represent the mean response magnitude (given by the t -value versus baseline) for all six stimulus categories in MPCv of both hemispheres. These responses have been rank ordered from strongest (i.e. closest to baseline) to weakest. Single participant data points are shown for each category. Gray lines depict pairwise-comparisons that survived Bonferroni correction ($p < 0.01$). The response to scenes was significantly different compared to all other categories in both hemispheres. **b.** Bars represent the mean response magnitude for all six stimulus categories in MPCd of both hemispheres. Bars are in the same order as in **a**, to highlight the different response profiles. Gray lines depict pairwise-comparisons that survived Bonferroni correction ($p < 0.01$). The response to faces was significantly different from the majority of the other categories.

Fig. 3: Memory task schematic and average BOLD responses to all conditions in MPC subdivisions. **a.** During the memory task, participants were given trial-wise instructions to recall from memory either famous people, famous places, personally familiar people or personally familiar places, respectively. Participants were asked to visualize the trial target from memory as vividly as possible for the duration of the trial (10 s). Trials were separated by a variable inter-trial-interval (2.5 -7.5 s). Participants completed 6 runs of the memory task. Each run contained 6 randomized trials from each condition. **b.** Average response curves from left and right MPCv (relative to baseline) are shown for all conditions in both hemispheres. Response curves were generated by first measuring the average response across the ROI for each trial (6 TR's from trial onset) and then averaging across trials of the same condition. These responses were then averaged across participants and plotted for each condition separately (Famous people – dashed blue, Famous places – dashed red, Personal people – solid blue and Personal places – solid red). MPCv is maximally recruited during the recall of personal places. The patterns of response are very similar across hemispheres. **c.** Same as **b**, but for MPCd. In contrast to **b**, MPCd is maximally recruited during the recall of personal people. Again, this pattern is consistent across hemispheres. Response curves were normalized to begin at baseline (zero) for each trial separately. Gray-lines represent the standard error of the mean (sem) across participants for each condition and TR.

Fig. 4: Magnitude of memory recall for all conditions in MPCv and MPCd. **a.** Bars represent the mean response magnitude for each condition (t -value versus baseline) in MPCv of both hemispheres (Famous people – blue open bars, Famous places – red open bars, Personal people – blue closed bars, Personal places – red closed bars). Data points for each participant are connected. In both hemispheres, MPCv is positively recruited during the recall of famous places and personal places, whereas responses during the recall of people (either famous or personal) are largely negative, reflecting a Category preference for places. MPCv also exhibits a familiarity effect and is maximally recruited during the recall of personal places, reflecting the effect of Familiarity. The interaction between Category and Familiarity is also evident. Indeed, there is a larger category difference (places-people) in the personal over famous conditions. **B.** Bars represent the mean response magnitude for each condition in MPCd of both hemispheres. Here, MPCd is only positively recruited during recall of personal people, reflecting both a Category preference for people and a Familiarity effect. The interaction between Category and Familiarity is also evident: there is a larger category difference (places-people) in the personal over famous conditions.

Fig. 5: Ventral/posterior – dorsal/anterior shift in peak place memory and peak people memory. Enlarged partial views of the posterior medial portion of both the left and right hemispheres are shown. Overlaid onto these enlarged surfaces are the locations of the peak responses during recall of personal places (red dots) and recall of personal people (blue dots) for each participant. The corresponding peaks are connected for each participant with a dashed black line. Across participants, there is a consistent ventral/posterior – dorsal/anterior shift in the peak location of memory recall, such that the peak for recall of personal places is never posterior or ventral of the peak for recall of personal people.

Fig. 6: Familiarity and Category-selective recall in MPC. **a.** Medial views of both the left and right hemispheres of a representative participant are shown. Overlaid onto these surfaces is the main effect of Category from the linear-mixed-effects analysis (node-wise $p = 1.0^{-4}$, $q = 5.8^{-4}$). Cold colors represent regions of the brain more active during the recall of people (famous and personal), whereas hot colors represent regions of the brain more active during recall of places (famous and personal). An alternating pattern of memory recall is evident within MPC along the ventral/posterior – dorsal/anterior axis. ROIs 1 and 2,

correspond largely to our initial resting-state ROIs (MPCv, MPCd), whereas the anterior pair of regions was not defined initially. We also observe significant place recall in aPPA, and some small clusters of significant people recall in anterior cingulate cortex. **b**, The same medial views are shown but overlaid is the main effect of Familiarity (node-wise $p=1.0^{-4}$, $q=5.8^{-4}$). Cold colors represent regions of the brain more active during the recall of personally familiar stimuli (places and people), whereas hot colors represent regions of the brain more active during the recall of famous stimuli (places or people). A large swath of MPC exhibits an overwhelming Familiarity effect with greater activity during recall of personal over famous stimuli. Familiarity effects were also present in the anterior cingulate cortex, insula and ventral medial prefrontal cortex.

Fig. 7: Split-half analysis and memory recall effects in four MPC subdivisions. **a**, The effect of Category (node-wise $p=1.0^{-4}$, $q=5.8^{-4}$) is overlaid onto medial views of both the left and right hemispheres for both independent halves of the data separately (Odd – top row, Even – bottom row). Cold colors represent regions of the brain more active during the recall of people, whereas hot colors represent regions of the brain more active during recall of places. Despite having half the amount of data, the alternating pattern of category-selectivity within MPC is present in both halves and hemispheres, respectively. The magnitude of the category effect (F-stat) was highly correlated across splits. The reported rho-values correspond to the correlation of the node-wise F-statistic for the effect of category in each hemisphere across the two splits. **b**, Bars represent the mean response magnitude for each condition (t-value versus baseline) from ROI 1. Single participant data points are shown and are connected for each participant. **c-e**, same as **a**, but for ROIs 2-4.

Fig. 8: People and Place memory areas of MPC correspond to the dorsal and ventral DMN subnetworks. **a**, Medial views of both the left and right hemispheres are shown (TT n27 surface). Overlaid onto these surfaces is the effect of Category ($p=1.0^{-4}$, $q=5.8^{-4}$). Cold colors represent regions of the brain more active during the recall of people (famous and personal), whereas hot colors represent regions of the brain more active during recall of places (famous and personal). Masks of the dorsal DMN (dDMN) are outlined in black and show a striking spatial correspondence to regions more active during recall of people. In contrast, masks of the ventral DMN (vDMN) are outlined in white and correspond to regions more active during recall of places. DMN masks were taken from 38. **b**, The effect of Familiarity is overlaid onto the same surfaces ($p=1.0^{-4}$, $q=5.8^{-4}$). Cold colors represent regions of the brain more active during the recall of personally familiar stimuli (places and people), whereas hot colors represent regions of the brain more active during the recall of famous stimuli (places or people). Unlike in **a**, regions showing a Familiarity effect overlap with regions from both the dDMN and vDMN.

Figure 6-figure supplement 1: Memory recall effects on the lateral surface. **a**, Lateral views of the left and right hemispheres are shown. Overlaid onto these surfaces is the main effect of Category ($p=1.0^{-4}$, $q=5.8^{-4}$). Cold colors represent regions of the brain more active during the recall of people (famous and personal), whereas hot colors represent regions of the brain more active during recall of places (famous and personal). Significant responses during place recall were present in the posterior angular gyrus, inferior temporal sulcus and superior frontal regions. In contrast, significant responses to people recall were generally smaller in areal extent but nevertheless present in the insula and anterior temporal regions, particularly in the right hemisphere. **b**, Effect of Familiarity ($p=1.0^{-4}$, $q=5.8^{-4}$) overlaid onto the same surfaces. Cold colors represent regions of the brain more active during the recall of personally familiar stimuli (places and people), whereas hot colors represent regions of the brain more active during the recall of famous stimuli (places or people). Familiarity effects were present in superior-frontal regions, superior-temporal sulcus and the angular gyrus/caudal inferior parietal lobule.

Figure 6-figure supplement 2: Memory recall effects in PPA and FFA **a**, Bars represent the mean magnitude of response (t-value versus baseline) for all conditions in PPA of both the left and right hemispheres. Single participant data points and are shown and are connected for each participant. PPA is positively engaged during the recall of famous places and personal places, whereas responses during the recall of people (either famous or personal) are negative, reflecting a Category preference for places. PPA also exhibits a familiarity effect and is maximally engaged during the recall of personal places. The interaction between Category and Familiarity is also evident. Indeed, there is a larger category difference (places-people) in the personal over famous conditions. **b**, Same as **a**, but for FFA in both hemispheres. Unlike PPA, FFA is driven mostly by the recall of people but shows little to no effect of familiarity. Indeed, the response to famous and personal people is largely equivalent.

Figure 6-figure supplement 3: Memory recall effects in the Hippocampus and Amygdala. **a**, Axial, sagittal and coronal slices are shown. Overlaid onto these slices is the magnitude of the main effect of Familiarity. The red-circles highlight the approximate location of the Hippocampus in both hemispheres. Images are in radiological convention. Bars represent the mean magnitude of response to all conditions (versus baseline) in the Hippocampus of both the left and right hemispheres. Single participant data points and are shown and are connected for each participant. In both hemispheres, the Hippocampus shows larger positive responses on average during the recall of places over people, as well as, a familiarity effect with larger responses during recall of personal over famous stimuli. **b**, Axial, sagittal and coronal slices are shown. Overlaid onto these slices is the magnitude of the main effect of Category. The red-circles highlight the approximate location of the Amygdala in both hemispheres. Images are in radiological convention. Bars represent the mean magnitude of response to all conditions (versus baseline) in the Amygdala of both the left and right hemispheres. Unlike the Hippocampus, the Amygdala shows only the effect of Category with positive responses to the recall of famous and personal people, but little to no effect of Familiarity.

Figure 7-figure supplement 1: Functional connectivity between MPC subdivisions and foveal/peripheral early visual cortex. **a**, A posterior-medial view of the left hemisphere is shown with the foveal (purple) and peripheral (green) portions of early visual cortex highlighted. **b**, Bars represent the average functional connectivity between MPC places and both eccentricity representations in both hemispheres. Single participant data points and are shown and are connected for each participant. As predicted, MPC places shows on average stronger functional connectivity with peripheral over foveal portions of early visual cortex. **c**, same as **b**,

but for MPC people. In contrast, MPC people shows on average stronger functional connectivity with foveal over peripheral portions of early visual cortex. ns = $p > 0.05$, * $p < 0.05$, *** $p < 0.001$.

Materials and Methods

Participants

Participants for all experiments were recruited from the DC area and NIH community. All participants were right-handed with normal or corrected-to-normal vision and neurologically healthy. All participants gave written informed consent according to procedures approved by the NIH Institutional Review Board (protocol 93-M-0170, clinical trials # NCT00001360). Participants were monetarily compensated for their time.

Resting-state functional connectivity experiment: Sixty-five participants (40 female, mean age = 24.67 ± 3.2 years) completed the resting-state functional connectivity experiment.

Six category functional Localizer experiment: Twenty-nine participants (21 female, mean age = 24.2 years) completed the functional localizer experiment.

Memory experiment: Twenty-four participants (17 female, mean age = 24.2 years) completed the memory experiment. The sample size for the memory experiment was based on prior work from our group (Silson et al., 2019) employing a very similar paradigm.

Stimuli and Tasks

Six category functional localizer experiment: Participants completed six functional localizer runs. During each run, color images from six stimulus categories (Scenes,

Faces, Bodies, Buildings, Objects and Scrambled Objects) were presented at fixation (5x5° of visual angle) in 16 s blocks (20 images per block [300ms per image, 500ms blank]). Each category was presented twice per run, with the order of presentation counterbalanced across participants and runs. Participants responded via MRI compatible button box whenever the same image appeared sequentially. Stimuli for this and the other in-scanner tasks were presented using PsychoPy software (Peirce 2007) (RRID:SCR_006571) from a Macbook Pro laptop (Apple Systems, Cupertino, CA).

Memory Experiment: Stimuli consisted of written names and words: 36 famous people, 36 famous places, 36 personally familiar people and 36 personally familiar places. The stimuli were provided by participants through a survey completed prior to the fMRI scan. Participants selected 36 known famous people and famous places from a list of 60 possible famous people (e.g., Tom Hanks, Angelina Jolie) and 92 possible famous places (e.g., Eiffel Tower, Times Square), and also provided the experimenters with the names of 36 people and 36 places that were personally familiar to them. Stimuli were presented in white 18-point Arial, all capital type against a black background.

During the task, on each trial participants were instructed to visualize the presented stimulus from memory as vividly as possible for the duration of the trial (10 s). Trials were separated by a variable inter-trial interval (2.5-7.5 s). In each of the six runs, there were six trials of each condition (famous people, famous places, personally familiar people and personally familiar places) presented in a randomized order, for a total of 24 trials per run (144 trials total).

696

697 *Post scan questionnaire:* After the scans were complete, participants completed a
698 questionnaire in which they rated how vividly they were able to visualize from memory
699 each stimulus presented during the memory runs. The stimuli were listed in the same
700 order they appeared during the Memory Experiment and were rated on a 4-point Likert
701 type scale (1 = not at all vivid; 4 = extremely vivid). If the participant could not visualize
702 the stimulus at all while in the scanner, they checked a box on the questionnaire.

703

704 *Functional imaging parameters*

705 Below we outline the imaging parameters for the three separate imaging experiments
706 included in the current manuscript. All scans were performed on a 3.0T GE 750MRI
707 scanner using a 32-channel head coil.

708

709 *Resting-state functional connectivity:* All functional images were acquired using a
710 BOLD-contrast sensitive three-echo echo-planar sequence (ASSET acceleration factor
711 = 2, TEs =14.9, 28.4, 41.9 ms, flip-angle = 65°, bandwidth = 250.000 kHz, FOV = 24 x
712 24 cm, acquisition matrix = 64 x 64, resolution = 3.4 x 3.4 x 3.4 mm, slice gap = 0.3 mm,
713 34 slices per volume covering the whole brain). Respiratory and cardiac traces were
714 recorded. Resting state scans lasted 21-minutes. The first 30 volumes were discarded
715 to control for the state of arousal during the initial stages of data acquisition, leaving 20
716 minutes (600 volumes) for resting state functional connectivity analysis. This procedure
717 has been used in other studies where long-duration resting state runs were collected.

718

Six category functional localizer: All functional images were acquired using a BOLD-contrast sensitive standard EPI sequence (TE=30 ms, TR=2 s, flip-angle = 65 degrees, FOV=192 mm, acquisition matrix = 64 x 64, resolution 2 x 2 x 2 mm, slice gap = 0.2mm, 37 slices covering the occipital and temporal lobes.

Memory experiment: All functional images were acquired using a BOLD-contrast sensitive three-echo echo-planar sequence (ASSET acceleration factor = 2, TEs = 12.5, 27.7, and 42.9 ms, flip angle = 75°, 64 x 64 matrix, in-plane resolution = 3.2 x 3.2 mm, slice thickness = 3.5 mm). Repetition times (TRs) and acquired slices varied across different task conditions to be consistent with relevant prior work for each task. The memory task used a 2500 ms TR, with 35 slices collected. All slices were collected obliquely and were manually aligned to the AC-PC axis.

fMRI data preprocessing

Data were preprocessed using AFNI (Cox 1996) (RRID: SCR_005927) for all experiments. Below we outline the preprocessing steps taken during each experiment.

Resting-state and memory experiments: The first 4 frames of each run were discarded to allow for T1 equilibration effects. Initial preprocessing steps for fMRI data were carried out on each echo separately. Slice-time correction was applied (3dTShift) and signal outliers were attenuated (3dDespike). Motion-correction parameters were estimated from the middle echo based on rigid-body registration of each volume to the first volume of the scan; these alignment parameters were then applied to the first and

third echo. Data from all three acquired echoes were then registered to each participants' T1 image and combined to remove additional thermal and physiological noise using multi-echo independent components analysis (Kundu et al. 2012; 2013). This procedure initially uses a weighted-average of the three echo times for each scan run to reduce thermal noise within each voxel. It subsequently performs a spatial ICA to separate time series components and uses the known properties of T_2^* signal decay to separate putatively neuronal BOLD components from putative noise components. This is accomplished by comparing each component to a model that assumes a temporal dependence in signal decay (i.e., that is "BOLD-like") and to a different model that assumes temporal independence (i.e., that is "non-BOLD-like"). Components with a strong fit to the former and a poor fit to the latter model are retained for subsequent analysis. This procedure was conducted using default options in AFNI's tedana.py function. ME-ICA processed data from each scan were then aligned across runs for each participant.

Six category functional localizer experiment: All images were motion corrected to the first image of the first run (3dVolreg), after removal of the appropriate 'dummy' volumes (8) to allow stabilization of the magnetic field. Following motion correction, images were spatially smoothed (3dmerge) using a 5mm full-width-half-maximum smoothing kernel.

fMRI data analysis

Resting-state functional connectivity winner-take-all analysis: Each participant's resting-state functional connectivity time series was aligned to the standard surface using

3dVol2Surf. We sought to assess the RSFC between VTC and MPC as a function of both the posterior-anterior and medial-lateral axes. The region of VTC we considered was longer in the posterior-anterior direction than it was wide in the medial-lateral direction and so we chose to sample it using a 3x2 ROI scheme. Accordingly, Six ROIs were defined that divided VTC along both the posterior-anterior and medial-lateral axes with respect to the mid-fusiform sulcus on a standard surface mesh that was aligned to the anatomy of an independent participant (not included in this study). The surface vertices within these ROIs were transformed into each individual participant's surface. This is standard for surface-based ROI analyses in AFNI (Saad & Reynolds, 2012).

The surface mesh used within SUMA contains a standard number of vertices, whilst also respecting an individual participant's specific gyral and sulcal pattern. Thus, drawing these regions based on the medial and lateral fusiform gyrus on the surface mesh provides highly accurate mapping of this anatomical landmark across participants (Saad & Reynolds, 2012).

For each participant, time series from these six ROIs were first extracted then scaled by the mean, before the unique connectivity of each parcel to the rest of the brain was calculated using multiple-regression. The "winning" parcel at each node was then determined by the maximum beta-value for each parcel (e.g. anterior medial VTC), and the selectivity index of the node was determined by subtracting the mean beta-values of all other parcels from the winning parcel (e.g. selectivity index = anterior medial VTC –

(middle medial VTC + posterior medial VTC + anterior lateral VTC + middle lateral VTC + posterior lateral VTC).

An alternative approach is to normalize the variance (z-score) in the time-series prior to running the winner-take-all analysis. This analysis produced qualitatively similar results to our original analysis and thus, we elected to keep our original definitions of MPCv/MPCd.

Six category functional localizer analysis: A general linear model (GLM) approach was also used to analyze the functional localizer data. Specifically, a response model was built by convolving a standard gamma function with a 16 s square wave for each condition and compared against the activation time courses using Generalized Least Square (GLSQ) regression. Motion parameters and four polynomials accounting for slow drifts were included as regressors of no interest. To derive the response magnitude per condition, *t*-tests were performed between the condition-specific beta estimates (normalized by the grand mean of each voxel for each run) and baseline.

Memory analysis: Analyses were conducted using a general linear model (GLM) and the AFNI programs 3dDeconvolve and 3dREMLfit. The data at each time point were treated as the sum of all effects thought to be present at that time point and the time series was compared against GLSQ model fit with REML estimation of the temporal auto-correlation structure. Responses were modeled by convolving a standard gamma function with a 10 s square wave for each condition of interest (Famous People,

810 Famous Places, Personal People and Personal Places). Estimated motion parameters
811 were included as additional regressors of non-interest, and fourth-order polynomials
812 were included to account for slow drifts in the MR signal over time. Significance was
813 determined by comparing the beta estimates for each condition (normalized by the
814 grand mean of each voxel for each run) against baseline.

815 *Sampling of data to the cortical surface:* In each participant, the analyzed functional
816 data were projected onto surface reconstructions of each individual participant's
817 hemispheres using the Surface Mapping with AFNI (SUMA) software. First, data were
818 aligned to high-resolution anatomical scans (align_epi_anat.py). Once aligned, these
819 data were projected onto the cortical surface (3dVol2Surf) and smoothed by a 2mm
820 FWHM Gaussian kernel.

821
822 *Linear mixed effects analysis:* To look at the whole brain memory effects we employed a
823 linear-mixed-effects model (3dLME) in each hemisphere separately. The model
824 comprised two factors: Category (Places, People) and Familiarity (Famous, Personal).
825 At the whole brain-level, we did not observe any significant interactions, but both robust
826 main effects were significant.

827
828 *Split-half analysis:* For each participant, the six memory runs were divided into Odd and
829 Even splits (3 runs each). In each split, we performed the same LME. At the whole
830 brain-level, we did not observe any significant interactions, but both robust main effects
831 were significant. Throughout MPC we observed 4 ROIs that showed an alternating
832 pattern of category-selective recall in both splits. To quantify these effects, we first

defined each region within a split (e.g. Odd) and then sampled the data from the other half (e.g. Even). To avoid any potential bias in node selection, this process was reversed, and the average computed.

Statistical Approach

Statistical analyses of both behavioral and functional data were performed using the SPSS software package (IBM). For all analyses we conducted repeated measures ANOVAs. When a significant three-way interaction was present, we performed two separate two-way ANOVAs to explore the nature of the interaction.

Acknowledgments

We thank members of the Laboratory of Brain and Cognition for helpful comments on earlier version of the manuscript. This research was supported by the Intramural Research Program of the NIMH.

Funding

This work was supported by the Intramural Research Program (ZIAMH002909) of the National Institutes of Health – National Institute of Mental Health Clinical Study Protocol 93 M-0170, NCT00001360.

References

References

- Andrews-Hanna, J. R., Reidler, J. S., Sepulcre, J., Poulin, R., & Buckner, R. L. (2010). Functional-anatomic fractionation of the brain's default network. *Neuron*, 65(4), 550-562.
- Andrews-Hanna, J. R., Smallwood, J., & Spreng, R. N. (2014). The default network and self-generated thought: component processes, dynamic control, and clinical relevance. *Annals of the New York Academy of Sciences*, 1316(1), 29-52.
- Arcaro, M. J., & Livingstone, M. S. (2017). A hierarchical, retinotopic proto-organization of the primate visual system at birth. *Elife*, 6, e26196.
- Arnott, S. R., Heywood, C. A., Kentridge, R. W., & Goodale, M. A. (2008). Voice recognition and the posterior cingulate: an fMRI study of prosopagnosia. *Journal of neuropsychology*, 2(1), 269-286.

Baldassano, C., Beck, D. M., & Fei-Fei, L. (2013). Differential connectivity within the parahippocampal place area. *Neuroimage*, 75, 228-237.

Baldassano, C., Esteva, A., Fei-Fei, L., & Beck, D. M. (2016). Two distinct scene processing networks connecting vision and memory. *eNeuro*, ENEURO-0178.

Bar, M., Aminoff, E. 2003. Cortical analysis of visual context. *Neuron*. 38:347-358.

Braga, R. M., & Buckner, R. L. (2017). Parallel interdigitated distributed networks within the individual estimated by intrinsic functional connectivity. *Neuron*, 95(2), 457-471.

Bzdok, D., Heeger, A., Langner, R., Laird, A. R., Fox, P. T., Palomero-Gallagher, N., ... & Eickhoff, S. B. (2015). Subspecialization in the human posterior medial cortex. *Neuroimage*, 106, 55-71.

Chen, J., Leong, Y. C., Honey, C. J., Yong, C. H., Norman, K. A., & Hasson, U. (2017). Shared memories reveal shared structure in neural activity across individuals. *Nature neuroscience*, 20(1), 115.

Chrastil, E. R. (2018). Heterogeneity in human retrosplenial cortex: A review of function and connectivity. *Behavioral neuroscience*, 132(5), 317.

Cox, R. W. (1996). AFNI: software for analysis and visualization of functional magnetic resonance neuroimages. *Computers and Biomedical research*, 29(3), 162-173.

Daitch, A. L., & Parvizi, J. (2018). Spatial and temporal heterogeneity of neural responses in human posteromedial cortex. *Proceedings of the National Academy of Sciences*, 115(18), 4785-4790.

Daselaar, S. M., Prince, S. E., & Cabeza, R. (2004). When less means more: deactivations during encoding that predict subsequent memory. *Neuroimage*, 23(3), 921-927.

Daselaar, S. M., Prince, S. E., Dennis, N. A., Hayes, S. M., Kim, H., & Cabeza, R. (2009). Posterior midline and ventral parietal activity is associated with retrieval success and encoding failure. *Frontiers in human neuroscience*, 3, 13.

Deen, B., Richardson, H., Dilks, D. D., Takahashi, A., Keil, B., Wald, L. L., Kanwisher, N., & Saxe, R. (2017). Organization of high-level visual cortex in human infants. *Nature communications*, 8, 13995.

Epstein, R. A. (2008). Parahippocampal and retrosplenial contributions to human spatial navigation. *Trends in cognitive sciences*, 12(10), 388-396.

Epstein, R. A., Parker, W. E., & Feiler, A. M. (2007). Where am I now? Distinct roles for parahippocampal and retrosplenial cortices in place recognition. *Journal of Neuroscience*, 27(23), 6141-6149.

Foster, B. L., & Parvizi, J. (2012). Resting oscillations and cross-frequency coupling in the human posteromedial cortex. *Neuroimage*, 60(1), 384-391.

Gainotti, G., Almonti, S., Di Betta, A. M., & Silveri, M. C. (1998). Retrograde amnesia in a patient with retrosplenial tumour. *Neurocase*, 4(6), 519-526.

Gilmore, A. W., Nelson, S. M., Chen, H. Y., & McDermott, K. B. (2018). Task-related and resting-state fMRI identify distinct networks that preferentially support remembering the past and imagining the future. *Neuropsychologia*, 110, 180-189.

Gilmore, A. W., Nelson, S. M., & McDermott, K. B. (2015). A parietal memory network revealed by multiple MRI methods. *Trends in cognitive sciences*, 19(9), 534-543.

Gilmore, A. W., Nelson, S. M., & McDermott, K. B. (2014). The contextual association network activates more for remembered than for imagined events. *Cerebral Cortex*, 26(2), 611-617.

Gordon, E. M., Laumann, T. O., Gilmore, A. W., Newbold, D. J., Greene, D. J., Berg, J. J., ... & Hampton, J. M. (2017). Precision functional mapping of individual human brains. *Neuron*, 95(4), 791-807.

Hassabis, D., Kumaran, D., Maguire, E. A. 2007. Using imagination to understand the neural basis of episodic memory. *J Neurosci*. 27:14365-14374. 10.1523/JNEUROSCI.4549-07.2007.

Kanwisher, N., McDermott, J., & Chun, M. M. (1997). The fusiform face area: a module in human extrastriate cortex specialized for face perception. *Journal of neuroscience*, 17(11), 4302-4311.

Kim, H. (2013). Differential neural activity in the recognition of old versus new events: An activation likelihood estimation meta-analysis. *Human Brain Mapping*, 34(4), 814-836.

Konkle, T., & Caramazza, A. (2013). Tripartite organization of the ventral stream by animacy and object size. *Journal of Neuroscience*, 33(25), 10235-10242.

Konkle, T., & Oliva, A. (2012). A real-world size organization of object responses in occipitotemporal cortex. *Neuron*, 74(6), 1114-1124.

Kuhl, B. A., & Chun, M. M. (2014). Successful remembering elicits event-specific activity patterns in lateral parietal cortex. *Journal of Neuroscience*, 34(23), 8051-8060.

Kundu, P., Inati, S. J., Evans, J. W., Luh, W. M., & Bandettini, P. A. (2012). Differentiating BOLD and non-BOLD signals in fMRI time series using multi-echo EPI. *Neuroimage*, 60(3), 1759-1770.

924 Kundu, P., Brenowitz, N. D., Voon, V., Worbe, Y., Vértes, P. E., Inati, S. J., & Bullmore, E. T. (2013).
 925 Integrated strategy for improving functional connectivity mapping using multiecho fMRI. *Proceedings of*
 926 *the National Academy of Sciences*, 201301725.
 927 Leech, R., Kamourieh, S., Beckmann, C. F., & Sharp, D. J. (2011). Fractionating the default mode
 928 network: distinct contributions of the ventral and dorsal posterior cingulate cortex to cognitive
 929 control. *Journal of Neuroscience*, 31(9), 3217-3224.
 930 Levy, I., Hasson, U., Avidan, G., Hendler, T., & Malach, R. (2001). Center–periphery organization of
 931 human object areas. *Nature neuroscience*, 4(5), 533.
 932 Livingstone, M. S., Arcaro, M. J., & Schade, P. F. (2019). Cortex Is Cortex: Ubiquitous Principles Drive
 933 Face-Domain Development. *Trends in cognitive sciences*, 23(1), 3-4.
 934 Martin, A. (2016). GRAPES—Grounding representations in action, perception, and emotion systems:
 935 How object properties and categories are represented in the human brain. *Psychonomic bulletin &*
 936 *review*, 23(4), 979-990.
 937 Margulies, D. S., Ghosh, S. S., Goulas, A., Falkiewicz, M., Huntenburg, J. M., Langs, G., ... & Jefferies, E.
 938 (2016). Situating the default-mode network along a principal gradient of macroscale cortical
 939 organization. *Proceedings of the National Academy of Sciences*, 113(44), 12574-12579.
 940 McDermott, K. B., Ojemann, J. G., Petersen, S. E., Ollinger, J. M., Snyder, A. Z., Akbudak, E., ... &
 941 Raichle, M. E. (1999). Direct comparison of episodic encoding and retrieval of words: an event-related
 942 fMRI study. *Memory*, 7(5-6), 661-680.
 943 McDermott KB, Gilmore AW, Nelson SM, Watson JM, Ojemann JG. (2017). The parietal memory network
 944 activates similarly for true and associative false recognition elicited via the DRM procedure. *Cortex* 87:96-
 945 107.
 946 Murphy, C., Wang, H. T., Konu, D., Lowndes, R., Margulies, D. S., Jefferies, E., & Smallwood, J. (2019).
 947 Modes of operation: A topographic neural gradient supporting stimulus dependent and independent
 948 cognition. *NeuroImage*, 186, 487-496.
 949 Murphy, C., Jefferies, E., Rueschemeyer, S. A., Sormaz, M., Wang, H. T., Margulies, D. S., & Smallwood,
 950 J. (2018). Distant from input: Evidence of regions within the default mode network supporting
 951 perceptually-decoupled and conceptually-guided cognition. *Neuroimage*, 171, 393-401.
 952 Nelson, S. M., McDermott, K. B., & Petersen, S. E. (2012). In favor of a 'fractionation' view of ventral
 953 parietal cortex: comment on Cabeza et al. *Trends in Cognitive Sciences*, 16(8), 399-400.
 954 Parkinson, C., Kleinbaum, A. M., & Wheatley, T. (2017). Spontaneous neural encoding of social network
 955 position. *Nature Human Behaviour*, 1(5), 0072.
 956 Parvizi, J., Van Hoesen, G. W., Buckwalter, J., & Damasio, A. (2006). Neural connections of the
 957 posteromedial cortex in the macaque. *Proceedings of the National Academy of Sciences*, 103(5), 1563-
 958 1568.
 959 Peer, M., Salomon, R., Goldberg, I., Blanke, O., & Arzy, S. (2015). Brain system for mental orientation in
 960 space, time, and person. *Proceedings of the National Academy of Sciences*, 112(35), 11072-11077.
 961 Peirce, J. W. (2007). PsychoPy—psychophysics software in Python. *Journal of neuroscience*
 962 *methods*, 162(1-2), 8-13.
 963 Power, J. D., Cohen, A. L., Nelson, S. M., Wig, G. S., Barnes, K. A., Church, J. A., & Petersen, S. E.
 964 (2011). Functional network organization of the human brain. *Neuron*, 72(4), 665-678.
 965 Raichle, M. E., MacLeod, A. M., Snyder, A. Z., Powers, W. J., Gusnard, D. A., & Shulman, G. L. (2001). A
 966 default mode of brain function. *Proceedings of the National Academy of Sciences*, 98(2), 676-682.
 967 Ranganath, C., & Ritchey, M. (2012). Two cortical systems for memory-guided behaviour. *Nature*
 968 *Reviews Neuroscience*, 13(10), 713.
 969 Saad, Z. S., & Reynolds, R. C. (2012). Suma. *Neuroimage*, 62(2), 768-773.
 970 Shirer, W. R., Ryali, S., Rykhlevskaia, E., Menon, V., & Greicius, M. D. (2012). Decoding subject-driven
 971 cognitive states with whole-brain connectivity patterns. *Cerebral cortex*, 22(1), 158-165.
 972 Shmuel, A., Augath, M., Oeltermann, A., & Logothetis, N. K. (2006). Negative functional MRI response
 973 correlates with decreases in neuronal activity in monkey visual area V1. *Nature neuroscience*, 9(4), 569.
 974 Shmuel, A., Yacoub, E., Pfeuffer, J., Van de Moortele, P. F., Adriany, G., Hu, X., & Ugurbil, K. (2002).
 975 Sustained negative BOLD, blood flow and oxygen consumption response and its coupling to the positive
 976 response in the human brain. *Neuron*, 36(6), 1195-1210.
 977 Smith, A. T., Williams, A. L., & Singh, K. D. (2004). Negative BOLD in the visual cortex: evidence against
 978 blood stealing. *Human brain mapping*, 21(4), 213-220.

Silson, E. H., Chan, A. W. Y., Reynolds, R. C., Kravitz, D. J., & Baker, C. I. (2015). A retinotopic basis for the division of high-level scene processing between lateral and ventral human occipitotemporal cortex. *Journal of Neuroscience*, 35(34), 11921-11935.

Silson, E. H., Gilmore, A. W., Kalinowski, S. E., Steel, A., Kidder, A., Martin, A., & Baker, C. I. (2018). A posterior-anterior distinction between scene perception and scene construction in human medial parietal cortex. *Journal of Neuroscience*, 1219-18.

Silson, E. H., Steel, A. D., & Baker, C. I. (2016). Scene-selectivity and retinotopy in medial parietal cortex. *Frontiers in human neuroscience*, 10, 412.

Sugiura, M., Shah, N. J., Zilles, K., & Fink, G. R. (2005). Cortical representations of personally familiar objects and places: functional organization of the human posterior cingulate cortex. *Journal of cognitive neuroscience*, 17(2), 183-198.

Valenstein, E., Bowers, D., Verfaellie, M., Heilman, K. M., Day, A., & Watson, R. T. (1987). Retrosplenial amnesia. *Brain*, 110(6), 1631-1646.

Vidaurre, D., Abeyesuriya, R., Becker, R., Quinn, A. J., Alfaro-Almagro, F., Smith, S. M., & Woolrich, M. W. (2018). Discovering dynamic brain networks from big data in rest and task. *Neuroimage*, 180, 646-656.

Vilberg, K. L., & Rugg, M. D. (2008). Memory retrieval and the parietal cortex: a review of evidence from a dual-process perspective. *Neuropsychologia*, 46(7), 1787-1799.

Wagner, A. D., Shannon, B. J., Kahn, I., & Buckner, R. L. (2005). Parietal lobe contributions to episodic memory retrieval. *Trends in cognitive sciences*, 9(9), 445-453.

Weiner, K. S., Golarai, G., Caspers, J., Chuapoco, M. R., Mohlberg, H., Zilles, K., ... & Grill-Spector, K. (2014). The mid-fusiform sulcus: a landmark identifying both cytoarchitectonic and functional divisions of human ventral temporal cortex. *Neuroimage*, 84, 453-465.

Yeo BT, Krienen FM, Sepulcre J, Sabuncu MR, Lashkari D, Hollinshead M, Roffman JL, Smoller JW, Zöllei L, Polimeni JR, Fischl B, Liu H, Buckner RL. The organization of the human cerebral cortex estimated by intrinsic functional connectivity. *J Neurophysiol* 106: 1125–1165, 2011; doi:10.1152/jn.00338.2011.

1030
1031
1032
1033
1034
1035
1036
1037
1038
1039 Distinct subdivisions of human medial parietal cortex support recollection of places and
1040 people
1041

1042 Edward H. Silson*, Adam Steel*, Alexis Kidder, Adrian Gilmore & Chris I. Baker

1043 **Supplementary Material**

1044 **Supplementary File 1a:** Statistical analysis of behavioural responses collected directly after the memory
1045 experiment. Data are provided for both subjective vividness and the proportion of missed trials. Table
1046 includes F-values, degrees of freedom (*df*), *p*-values and estimates of effect size using partial eta
1047 squared. In each case, a two-way repeated measures ANOVA was conducted with Category (Places,
1048 People) and Familiarity (Famous, Personal) as within-participant factors. In the case of vividness ratings,
1049 both main effects of Category and Familiarity were significant, reflecting on average higher vividness
1050 ratings for the recall of people over places and for personal over famous stimuli. The significant Category
1051 by Familiarity interaction reflects a larger familiarity difference (Personal > Famous) during recall of places
1052 over people. For the proportion of missed trials, neither main effect was significant, but their interaction
1053 was. This interaction is driven by more missed trials for famous places than people, but fewer missed
1054 trials for personal scenes than people.

1055
1056
1057
1058
1059
1060
1061
1062
1063
1064
1065
1066
1067
1068
1069
1070
1071
1072
1073
1074
1075
1076
1077
1078

Linear mixed effects analysis

To look at the whole brain memory effects we employed a linear-mixed-effects model (3dLME) in each hemisphere separately. The model comprised two factors: Category (Places, People) and Familiarity (Famous, Personal).

Statistical analysis of memory recall effects within ROIs

The same procedure was adopted when assessing memory effects from all ROIs, whether defined using resting-state (e.g. MPCv, MPCd), via the split-half analysis (ROIs 1-4), Category-selectivity (e.g. PPA, FFA) or via anatomical selection (e.g. Hippocampus, Amygdala). In each case, the mean response to each condition (given by the *t*-value versus baseline) was calculated for each participant, ROI and hemisphere separately. These values were then subjected to a three-way repeated measures ANOVA with Category (Places, People) Familiarity (Famous, Personal) and Hemisphere (Left, Right) as within-participant factors. If a significant three-way interaction was observed, we further explored the nature of this interaction with two-way ANOVAs in each hemisphere separately. Below are the full statistical breakdowns.

Supplementary File 1b: Statistical analysis of memory effects in MPCv and MPCd. Table includes *F*-values, degrees of freedom (*df*), *p*-values and estimates of effect size using partial eta squared. MPCv showed significant main effects of Category, Familiarity and Hemisphere. These were qualified by a significant three-way interaction, reflecting a larger familiarity difference (Personal > Famous) between categories (Places > People) in the right over left hemisphere. MPCd also showed significant main effects but did not show a significant three-way interaction. Importantly, however, MPCd did show the predicted Category by Familiarity interaction, which reflects a larger familiarity difference for the recall of people over places.

Memory recall effects in the four MPC memory subdivisions

Of note, ROIs 1 and 2 although larger in areal extent shared considerable spatial overlap with our original resting-state definitions (ROI 1/MPCv proportional overlap, left=0.99, right=0.89; ROI 2/MPCd proportional overlap, left=0.55, right=0.67).

Supplementary File 1c: Statistical analysis of memory effects in ROI 1. Table includes *F*-values, degrees of freedom (*df*), *p*-values and estimates of effect size using partial eta squared. ROI 1 showed significant main effects of Category, Familiarity and Hemisphere. These were qualified by a significant three-way interaction, reflecting a larger familiarity difference (Personal > Famous) between categories (Places > People) in the right over left hemisphere.

Supplementary File 1d: Statistical analysis of memory effects in ROI 2. Table includes Fvalues, degrees of freedom (*df*), *p*-values and estimates of effect size using partial eta squared. ROI 2 showed significant main effects of Category, Familiarity and Hemisphere, but did not show a significant three-way interaction. Importantly, however, ROI 2 did show the predicted Category by Familiarity interaction, which reflects a larger familiarity difference for the recall of people over places.

Supplementary File 1e: Statistical analysis of memory effects in ROI 3. Table includes Fvalues, degrees of freedom (*df*), *p*-values and estimates of effect size using partial eta squared. ROI 3 showed significant main effects of Category, Familiarity, but not Hemisphere. Although ROI 3 did not show a significant three-way interaction, ROI 3 did show the predicted Category by Familiarity interaction, which reflects a larger familiarity difference for the recall of places over people.

Supplementary File 1f: Statistical analysis of memory effects in ROI 4. Table includes Fvalues, degrees of freedom (*df*), *p*-values and estimates of effect size using partial eta squared. ROI 4 showed significant main effects of Category, Familiarity and Hemisphere. These were qualified by a significant three-way interaction, reflecting a larger familiarity difference (Personal > Famous) between categories (People > Places) in the right over left hemisphere.

Memory recall effects in category-selective VTC

Given that participants were recalling specific places (i.e. scenes) and specific people (i.e. faces) we also looked within scene (PPA) and face (FFA) selective regions of VTC for possible memory effects. These ROIs were defined at the group-level based on the contrast of Scenes > Faces ($p=1.0^{-4}$).

Supplementary File 1g: Statistical analysis of memory effects in PPA and FFA. Table includes Fvalues, degrees of freedom (*df*), *p*-values and estimates of effect size using partial eta squared. PPA showed significant main effects of Category and Familiarity, but not Hemisphere. PPA only showed a significant Category by Familiarity interaction, reflecting a larger familiarity difference (Personal > Famous) between categories (Places > People) with no clear difference between hemispheres. In contrast, FFA showed significant main effects of Category and Hemisphere, but not Familiarity. These were qualified by a significant three-way interaction, which reflects the presence of category and familiarity in the left hemisphere, but only the effect of category in the right hemisphere.

Memory recall effects in Hippocampus and Amygdala

To better understand the memory recall effects observed in the Amygdala and Hippocampus detected at the group level, we sought to quantify these effects in individual participants using automatic parcellations of these structures in each participants' native anatomical space.

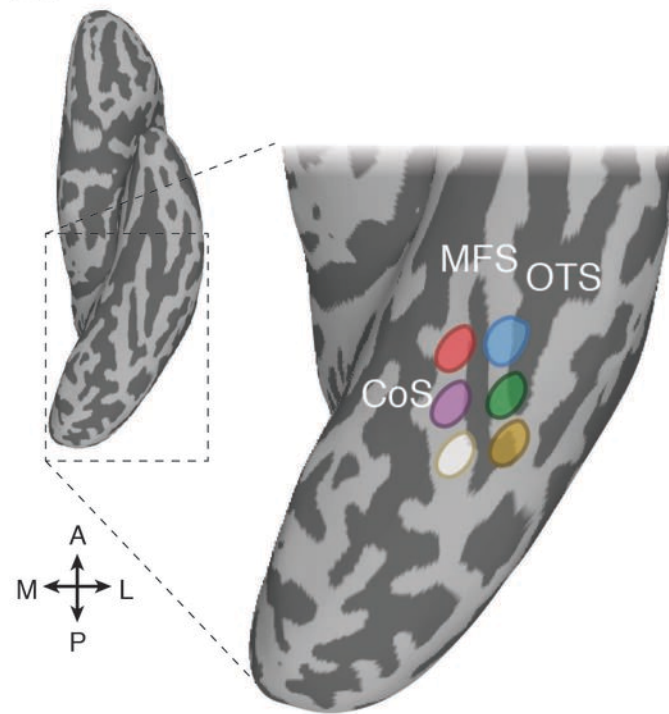
Supplementary File 1h: Statistical analysis of memory effects in the Hippocampus and Amygdala Table includes F-values, degrees of freedom (*df*), *p*-values and estimates of effect size using partial eta squared. The Hippocampus showed significant main effects of Category and Familiarity, but not Hemisphere. Only the Category by Hemisphere interaction was significant. The Amygdala showed only a significant effect of Category, with larger responses for the recall of people irrespective of the level of familiarity.

Functional connectivity with foveal and peripheral early visual cortex

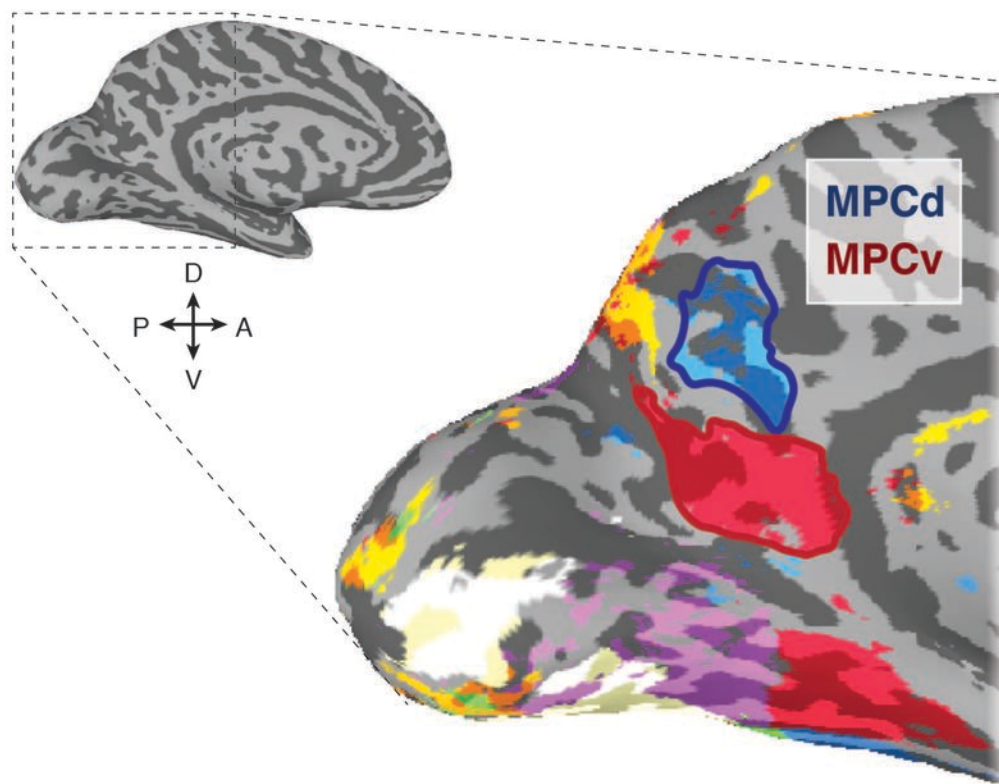
Given that category-preference and eccentricity are so highly correlated across the medial-lateral axis of VTC, we sought to test whether our initial MPC subdivisions would show stronger functional connectivity with foveal and peripheral portions of early visual cortex (EVC). Such a demonstration would provide further evidence for a functional link between VTC and MPC. Given the selective recruitment of MPCv during place recall, preference for scene stimuli and connectivity with medial VTC, we predicted stronger functional connectivity with peripheral over foveal portions of EVC. In contrast, given the selective recruitment of MPCd during people recall, preference for face stimuli and increased connectivity with medial VTC, we predicted the opposite pattern. To perform this analysis, we first defined foveal (0-4°) and peripheral (4-10°) regions of EVC in both hemispheres based on group retinotopic mapping data from a previous study from our group⁴³. Next, we calculated the average functional connectivity between our two MPC subdivisions and these different eccentricity representations.

Supplementary File 1i: Statistical analysis of the resting-state functional connectivity between MPCv, MPCd and Foveal, Peripheral portions of early visual cortex (EVC). Table includes F-values, degrees of freedom (*df*), *p*-values and estimates of effect size using partial eta squared. The main effects of ROI and Hemisphere were not significant, but the main effect of Eccentricity was reflecting on average stronger connectivity with peripheral than foveal portions of EVC. These were qualified however by a significant three-way interaction, reflecting on average stronger connectivity between MPCv and peripheral EVC, but stronger connectivity between MPCd and foveal EVC in the left over right hemispheres.

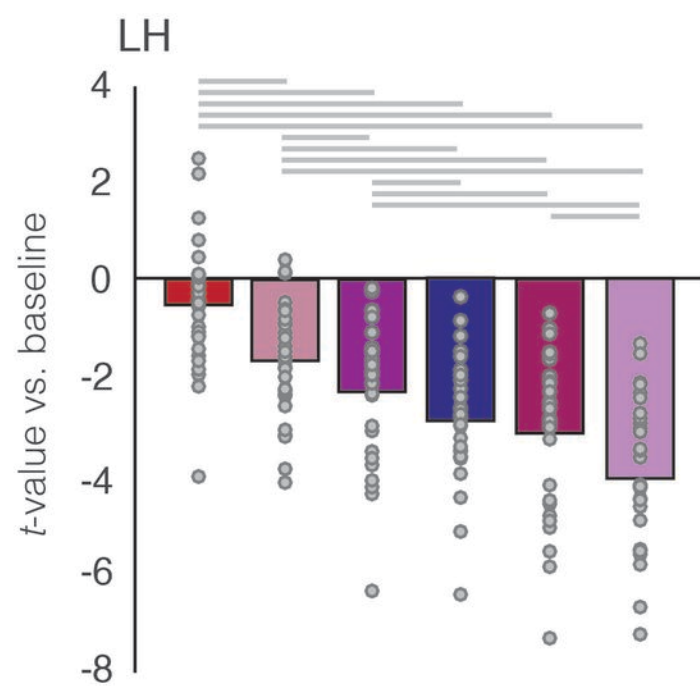
a



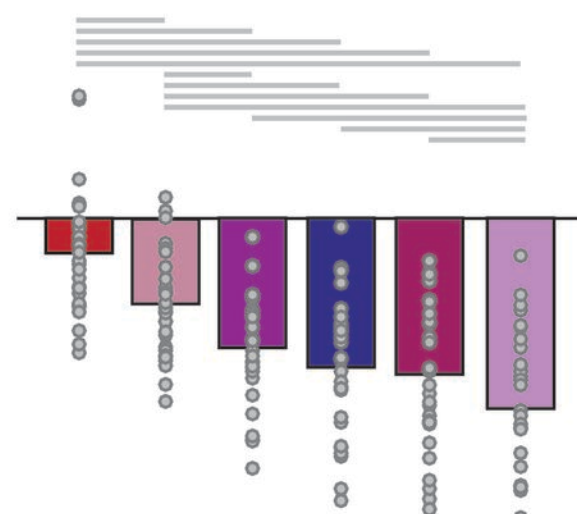
b



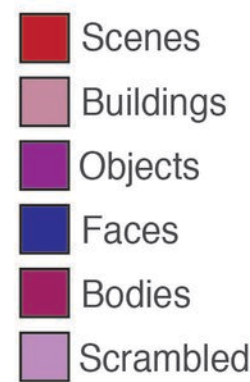
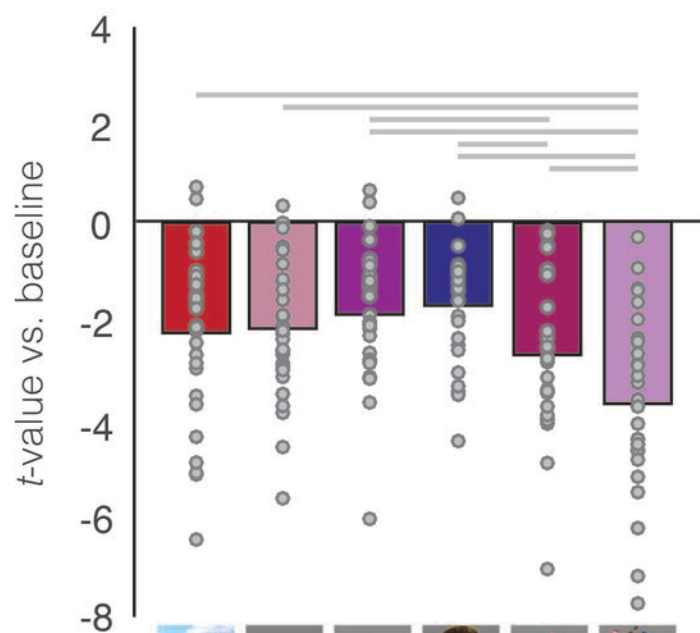
a
MPCv

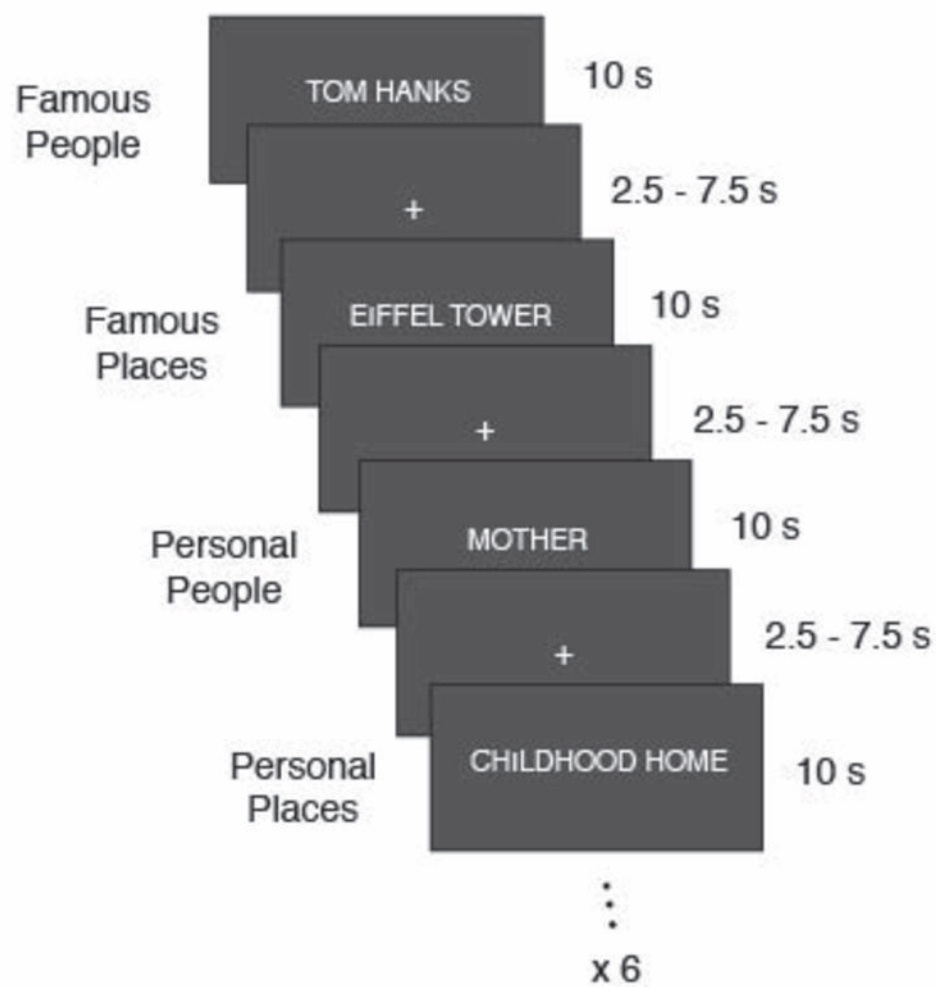
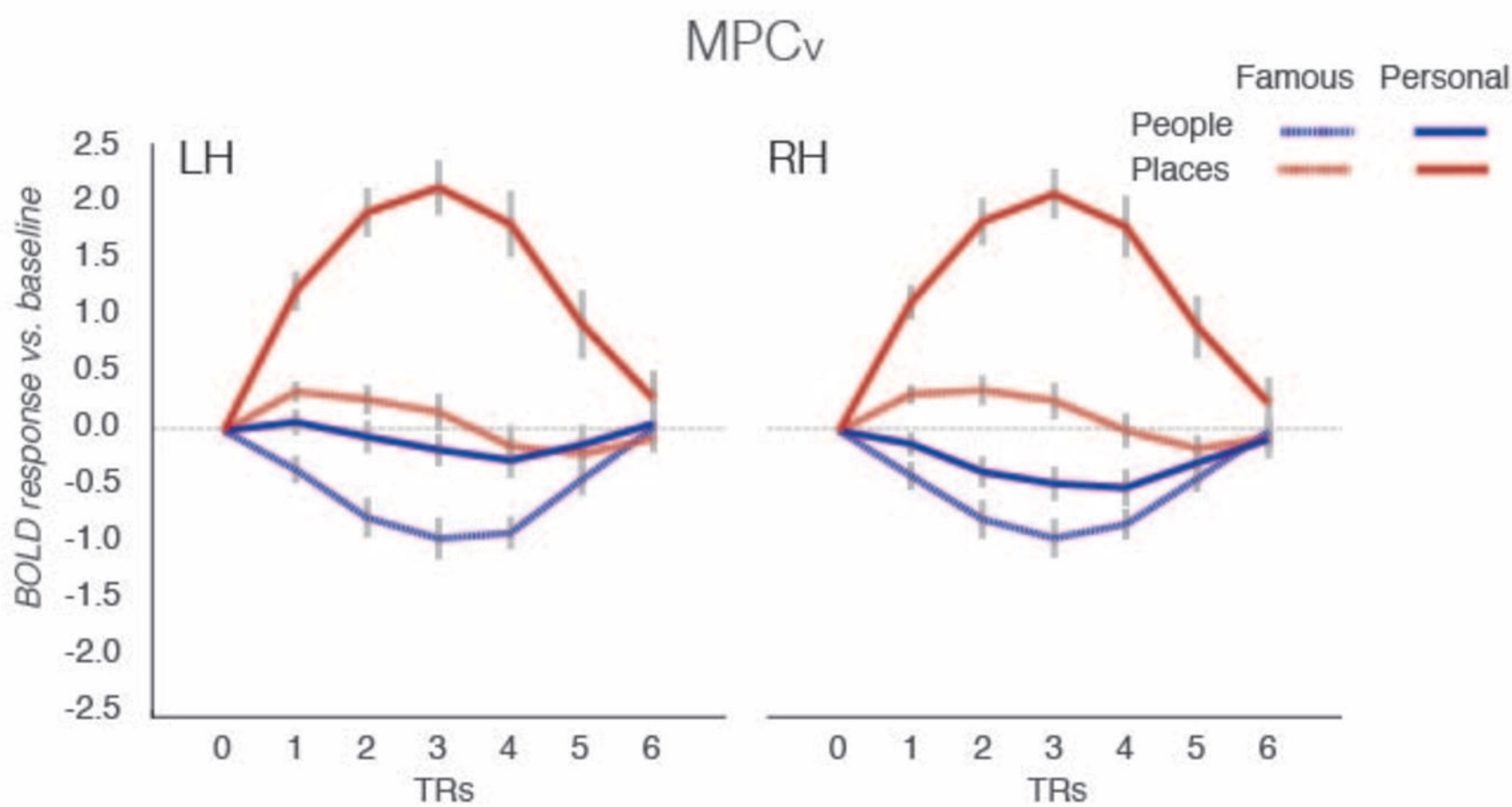
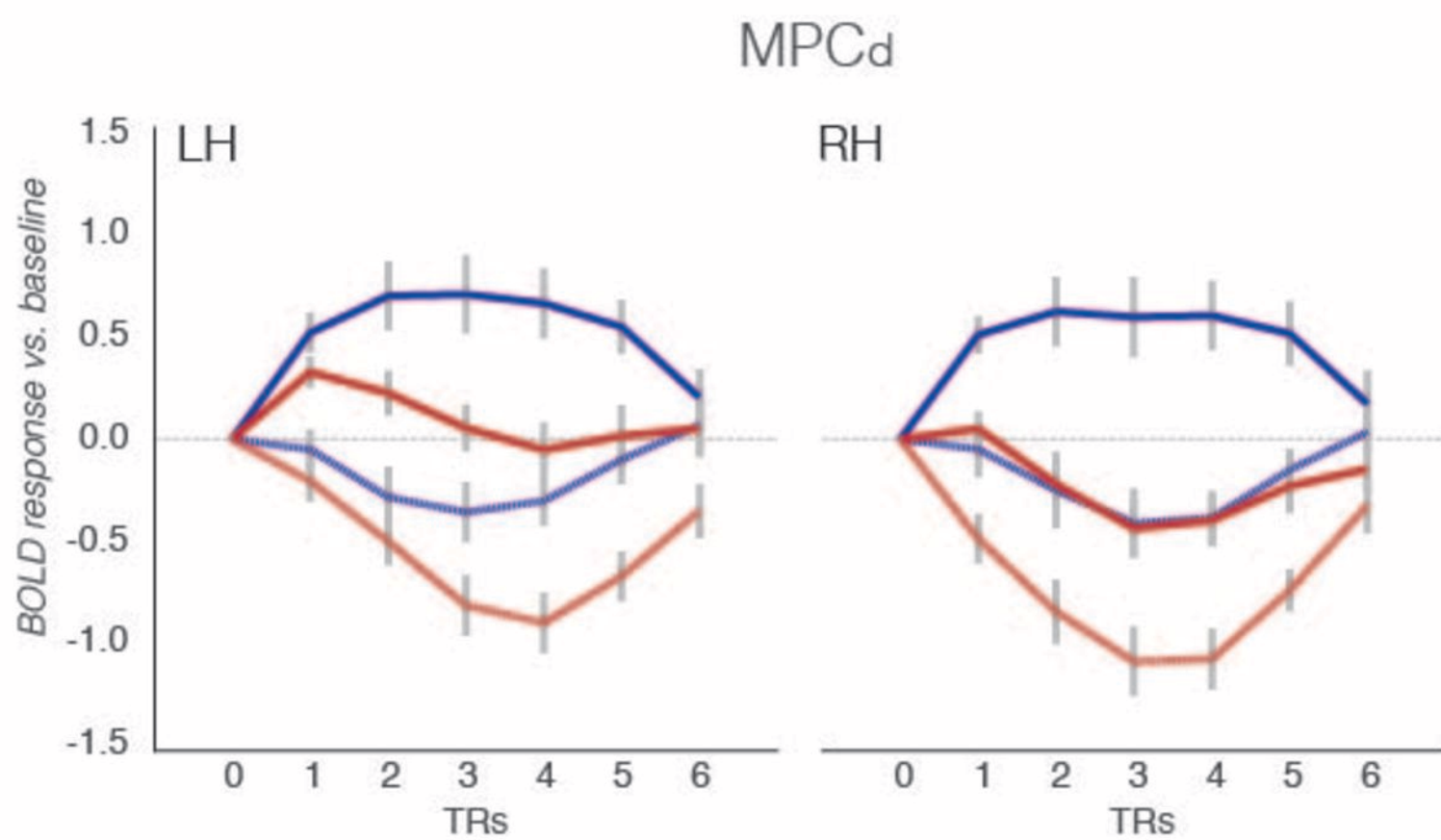


RH



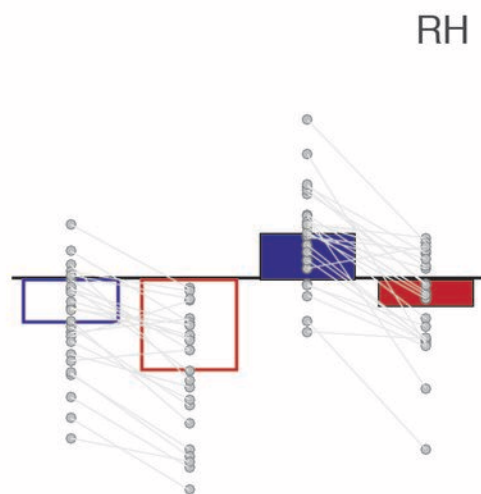
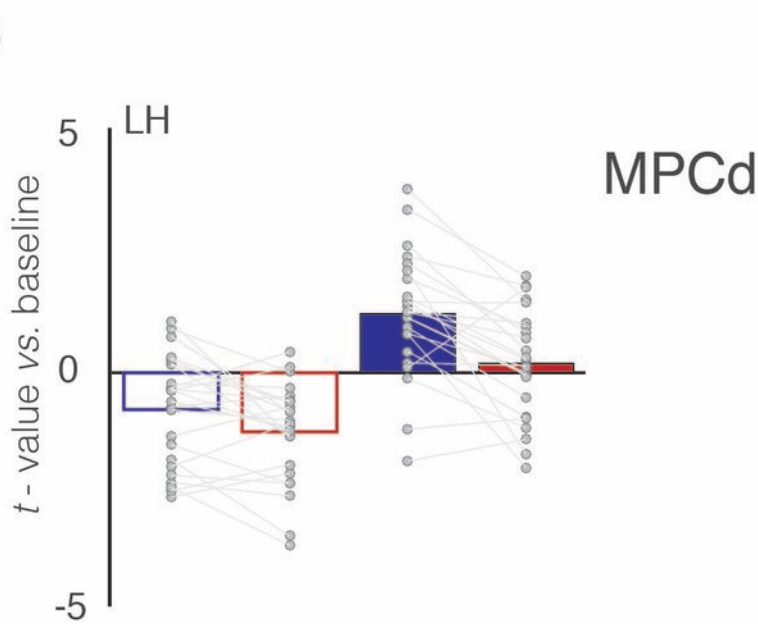
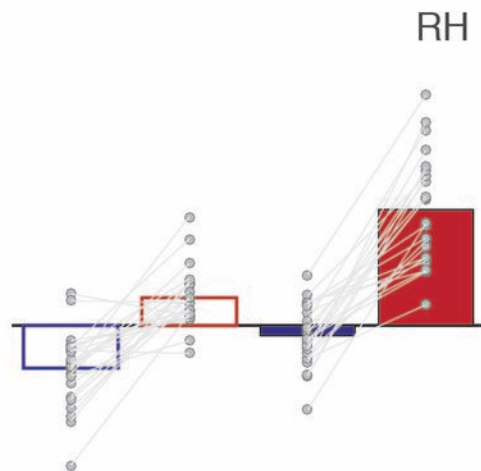
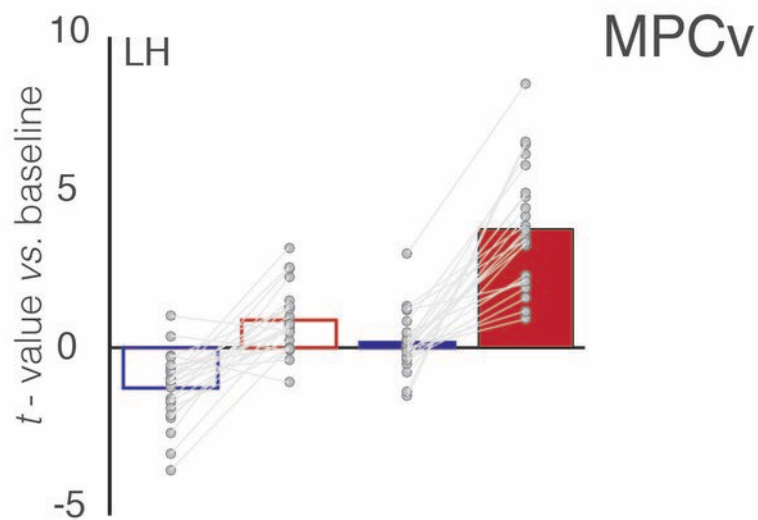
b
MPCd



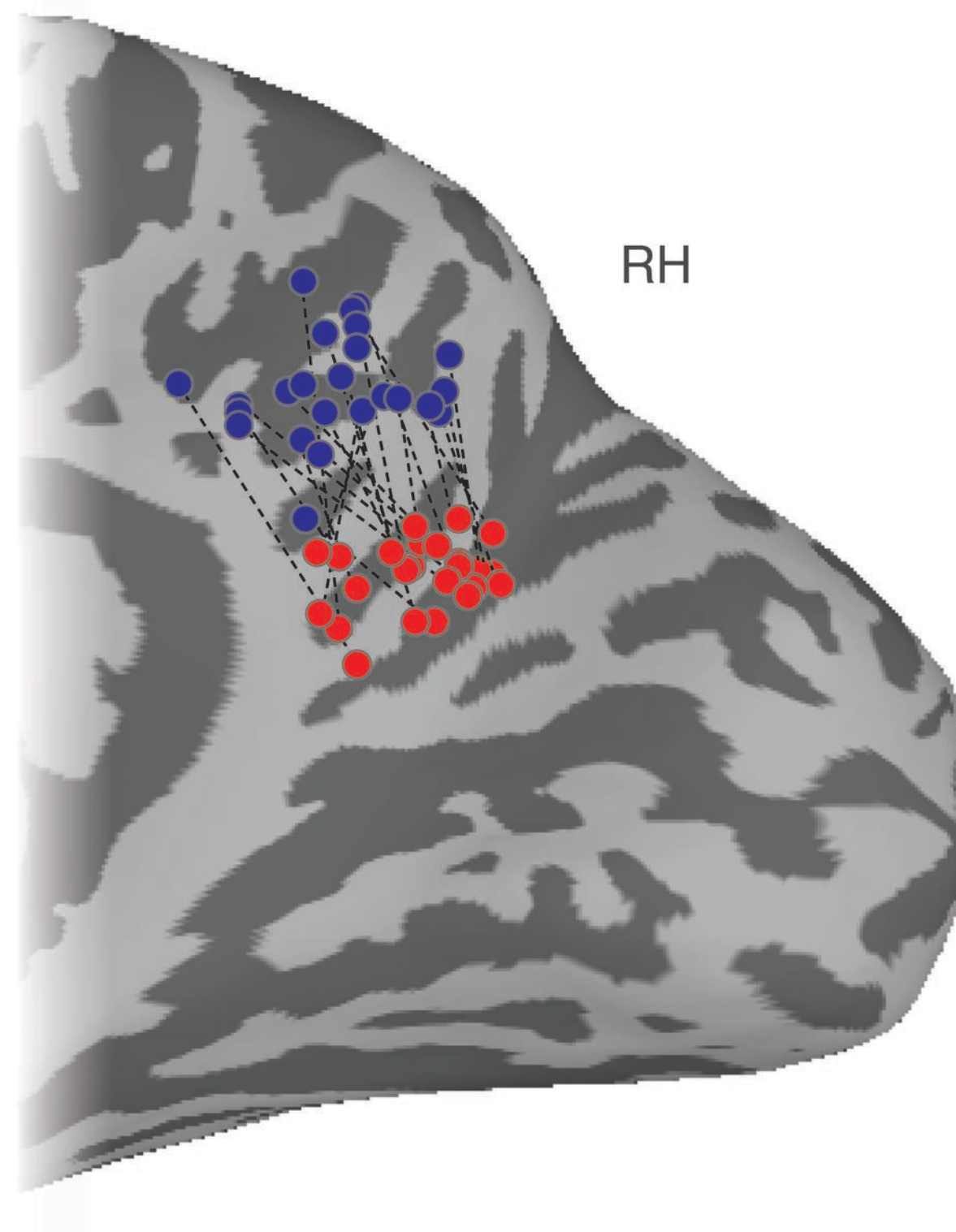
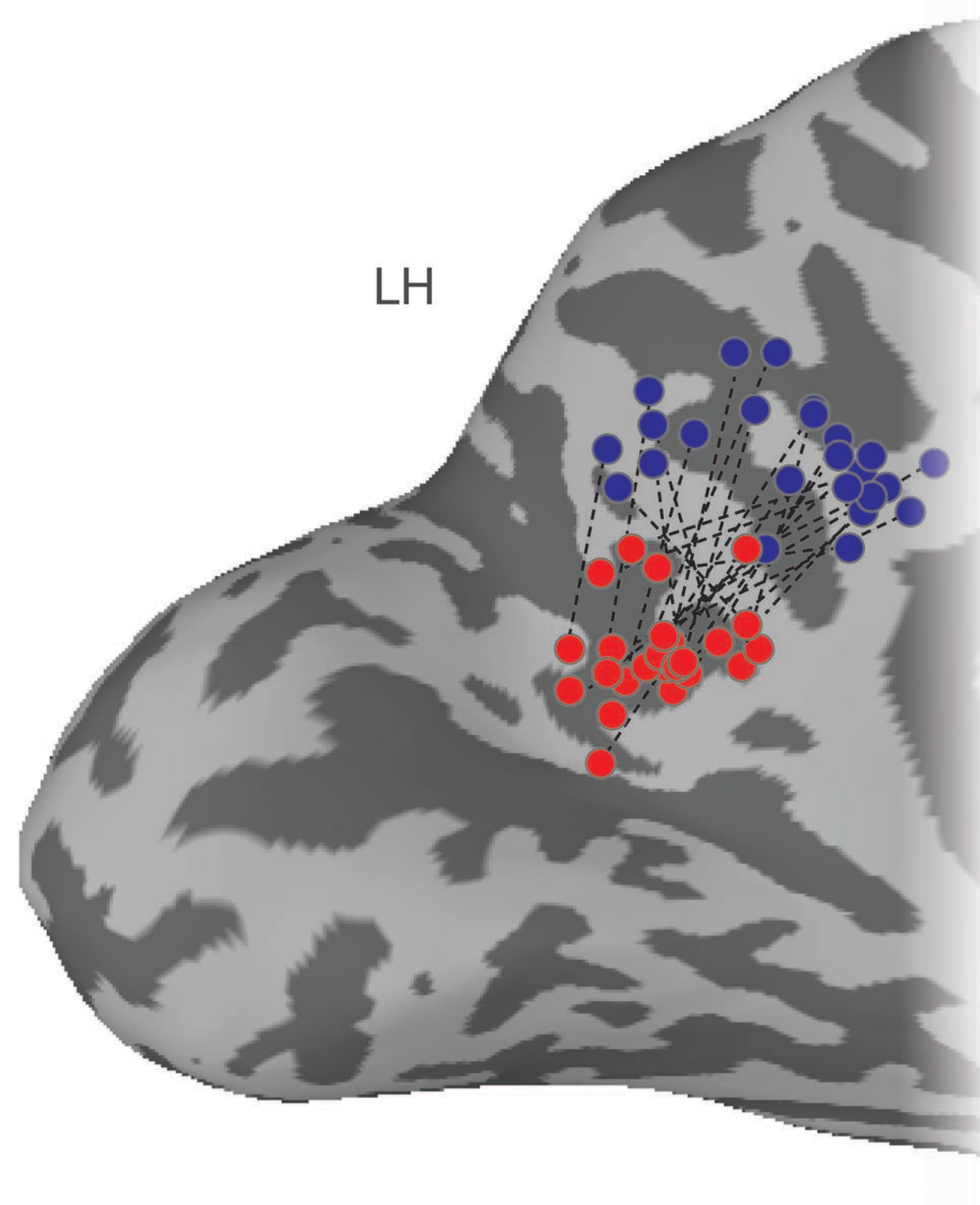
a**b****c**

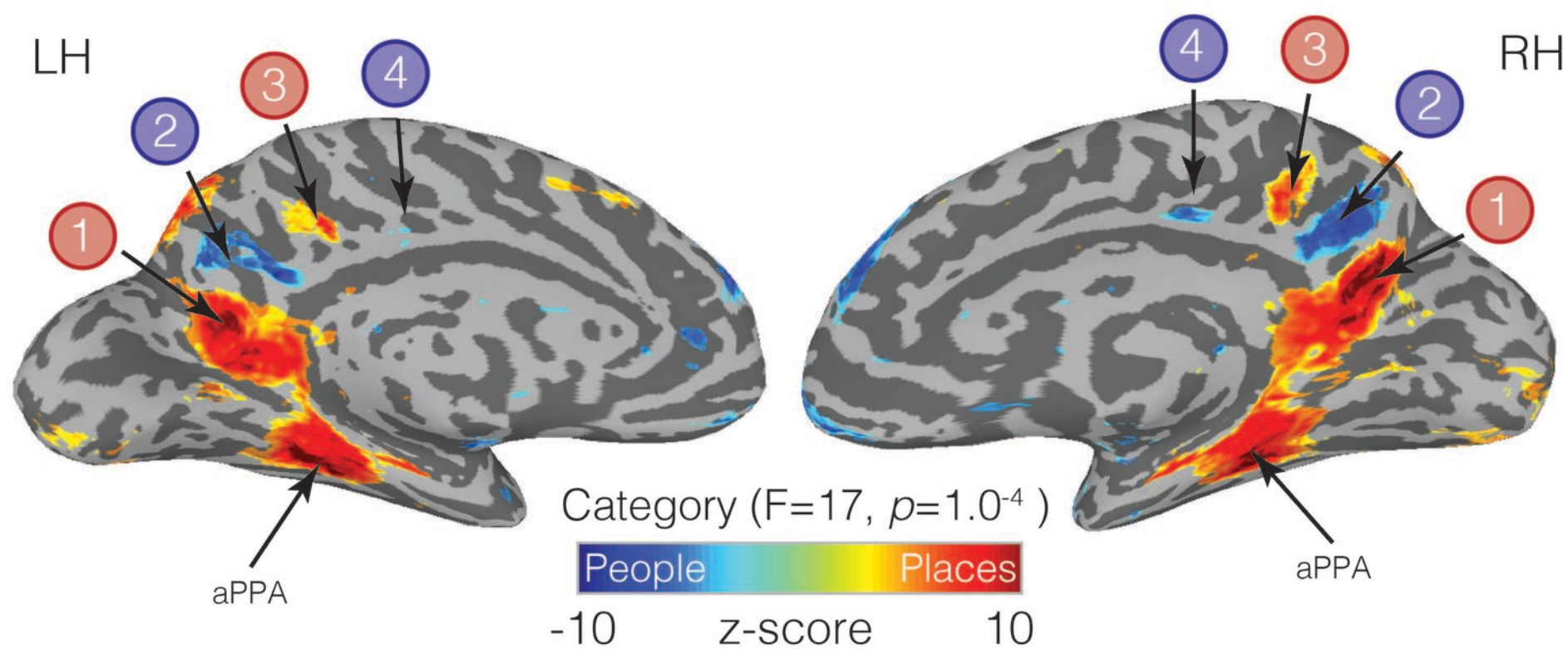
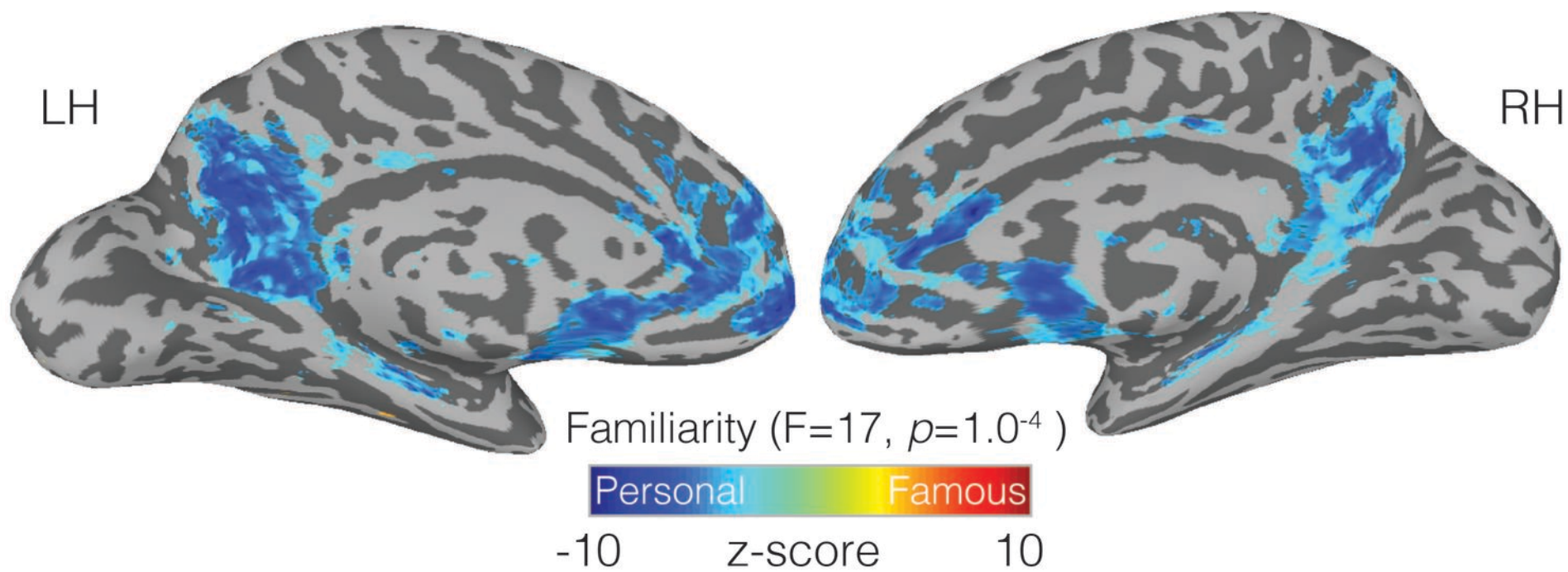
Famous Personal

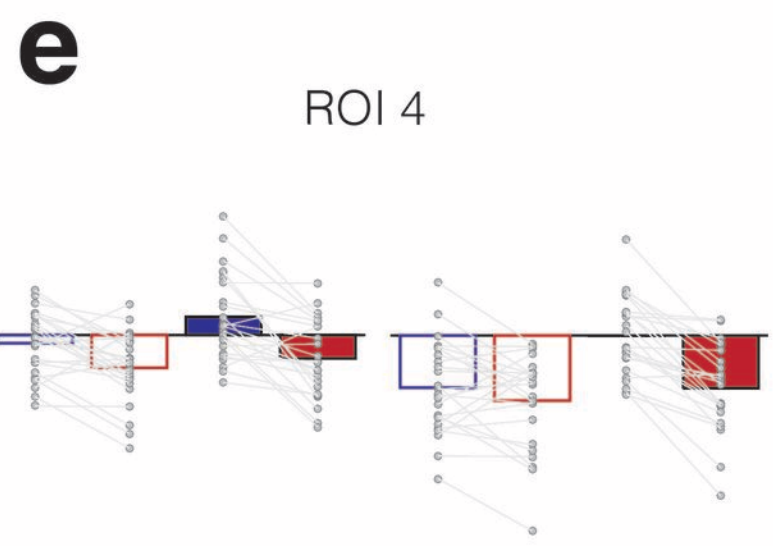
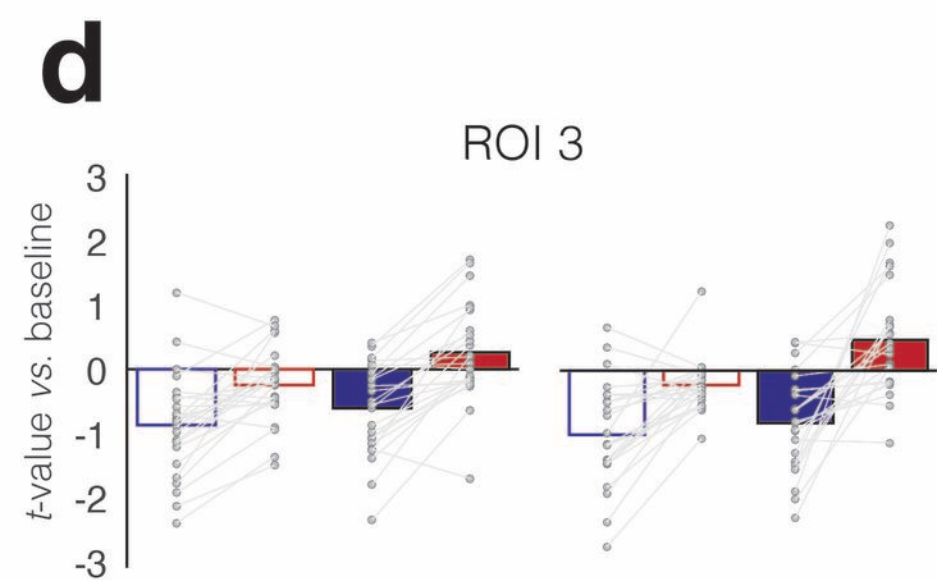
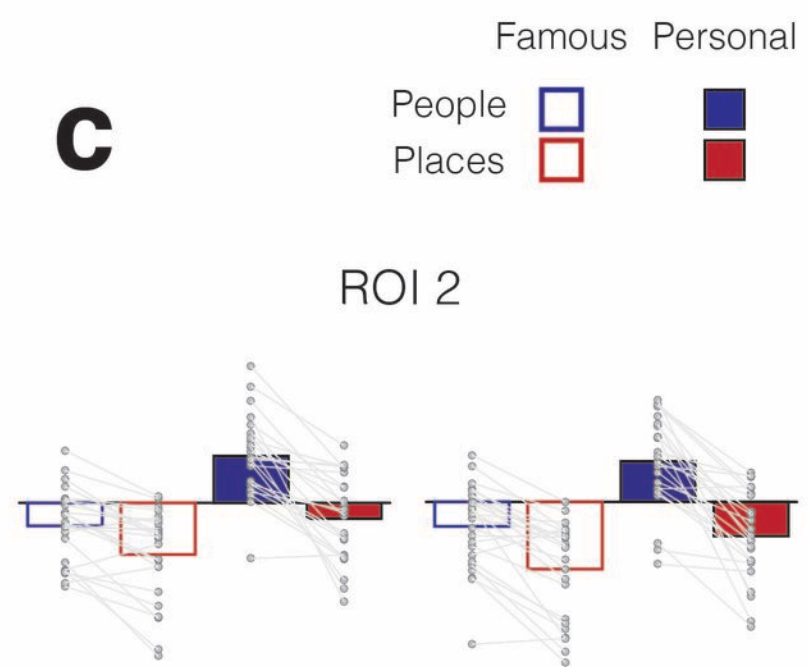
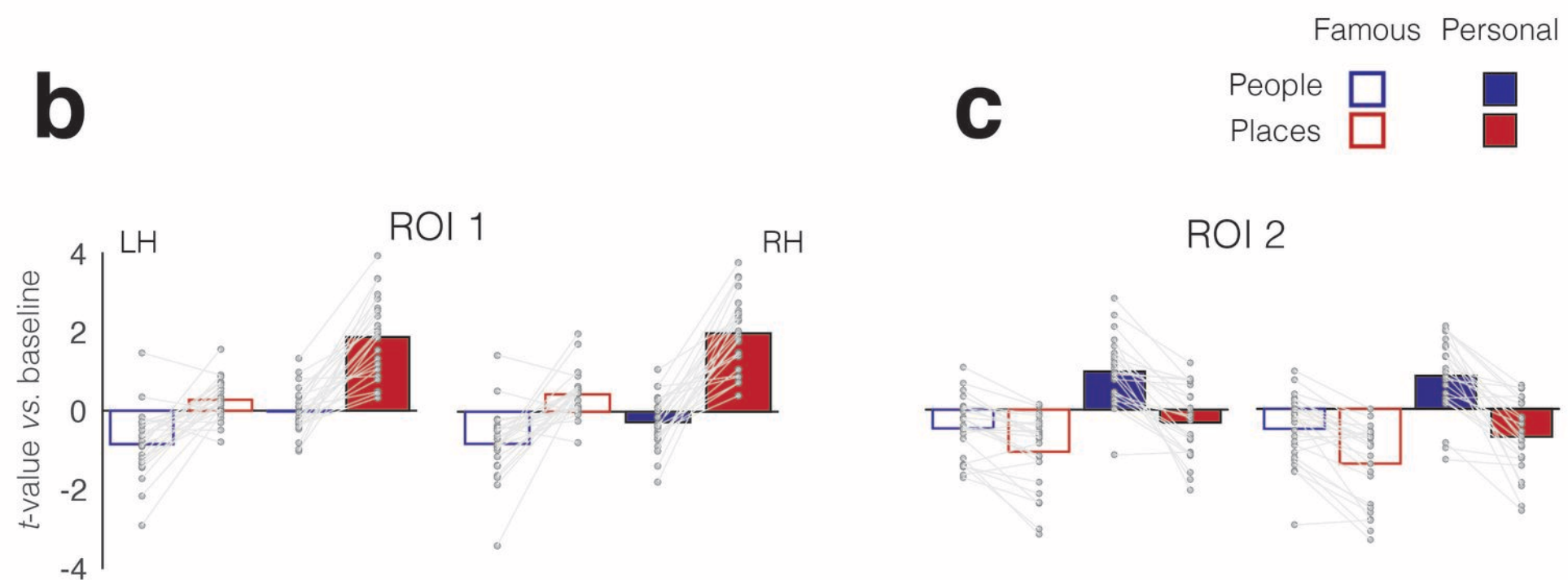
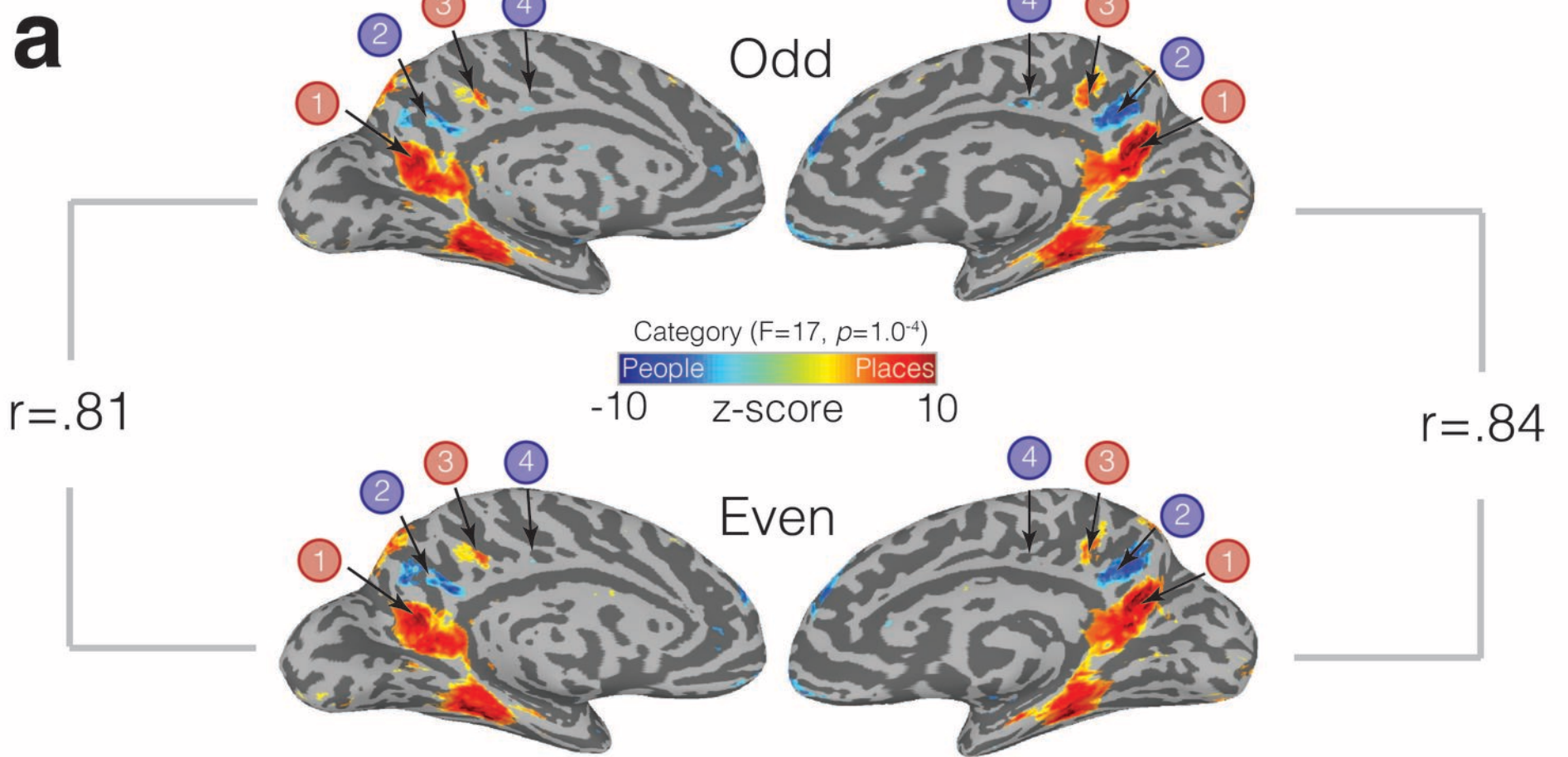
People
 Places

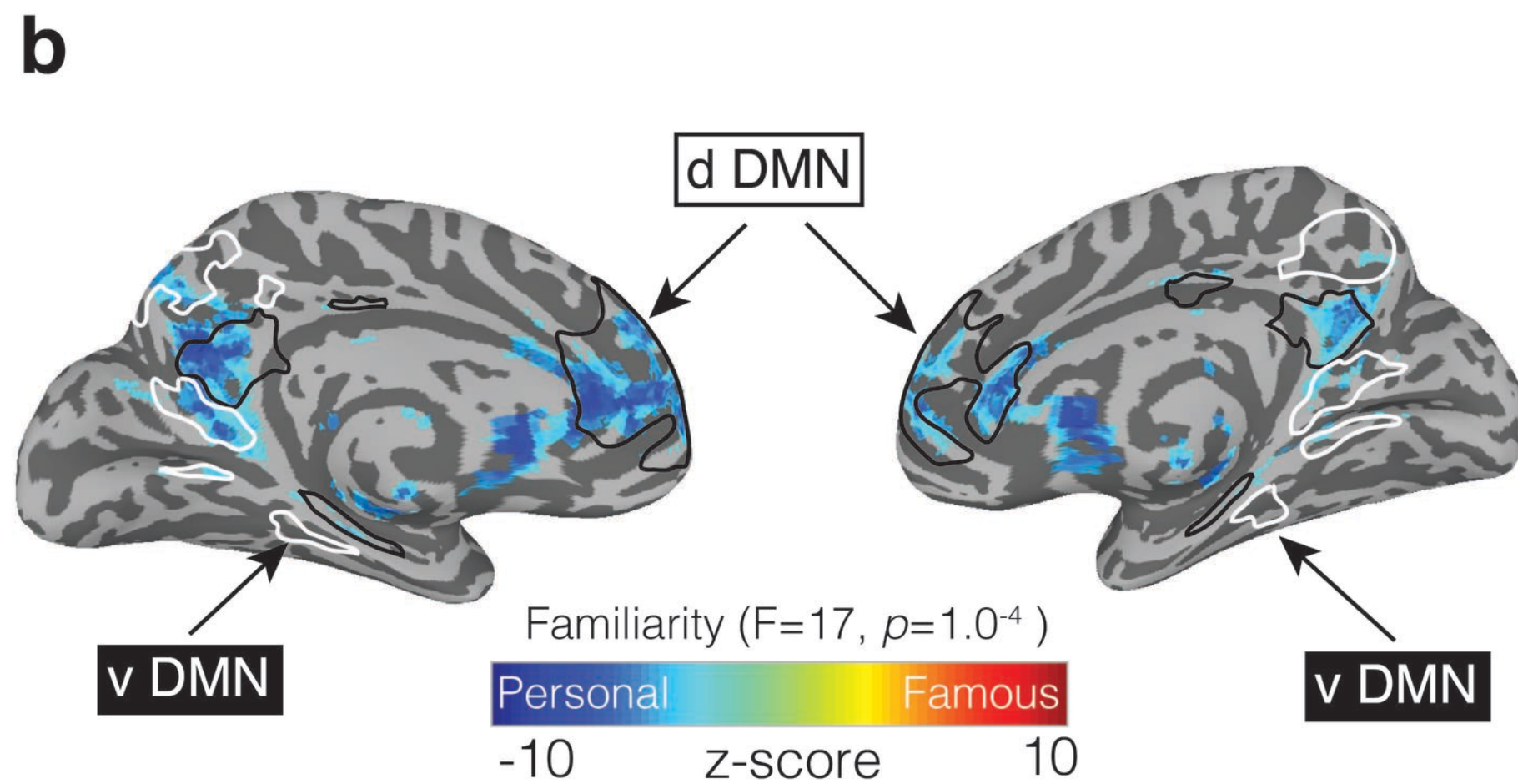
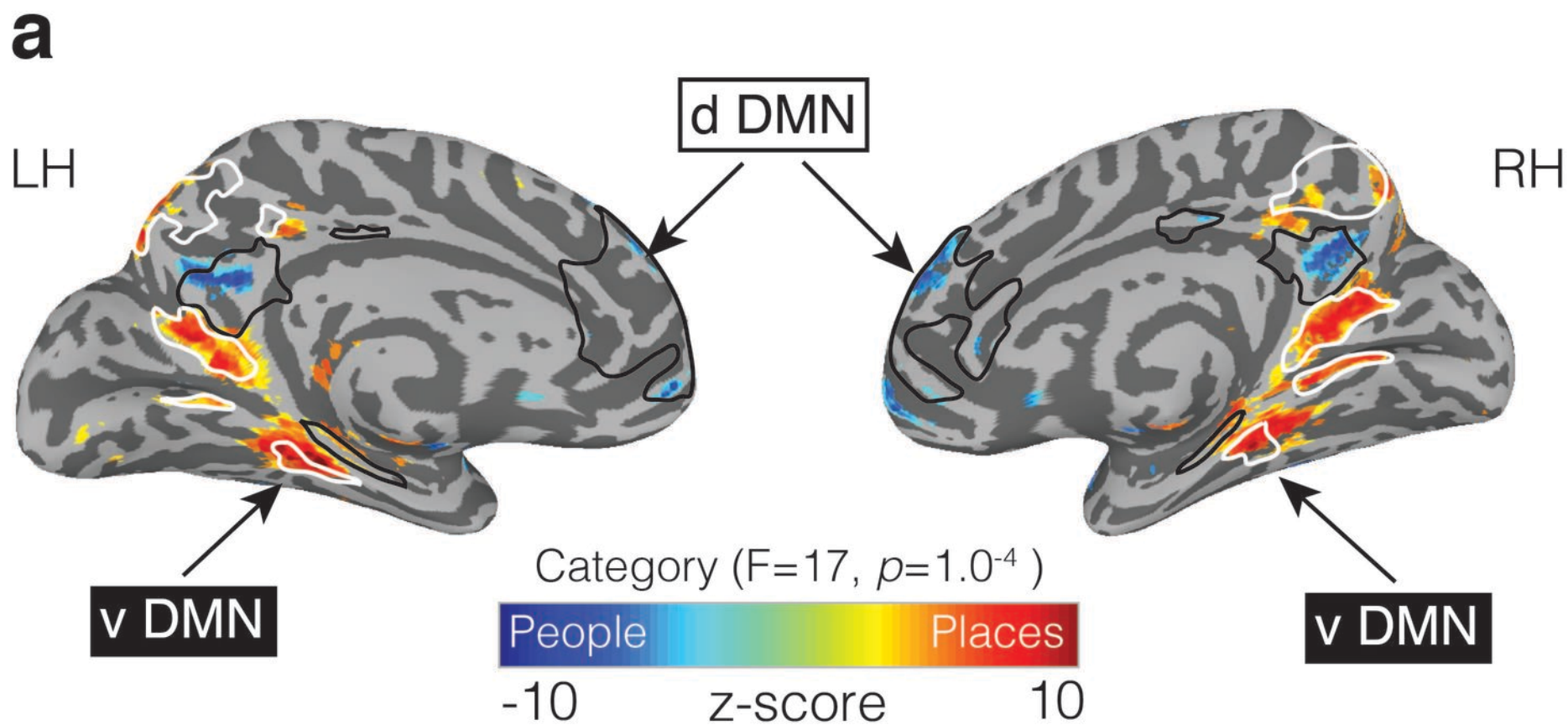


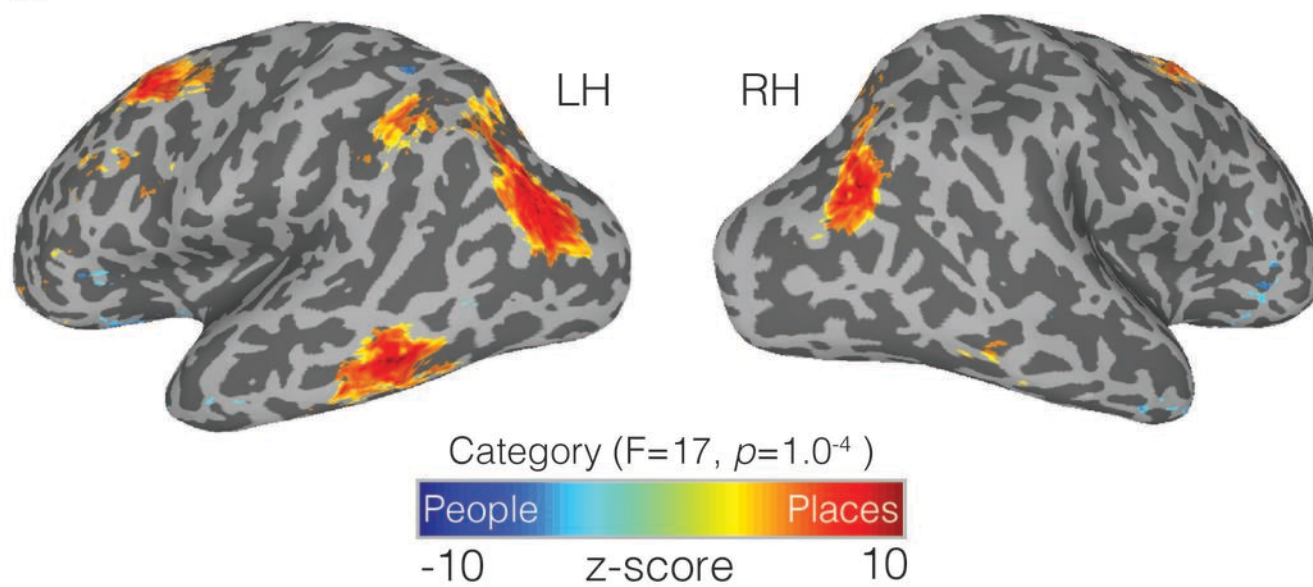
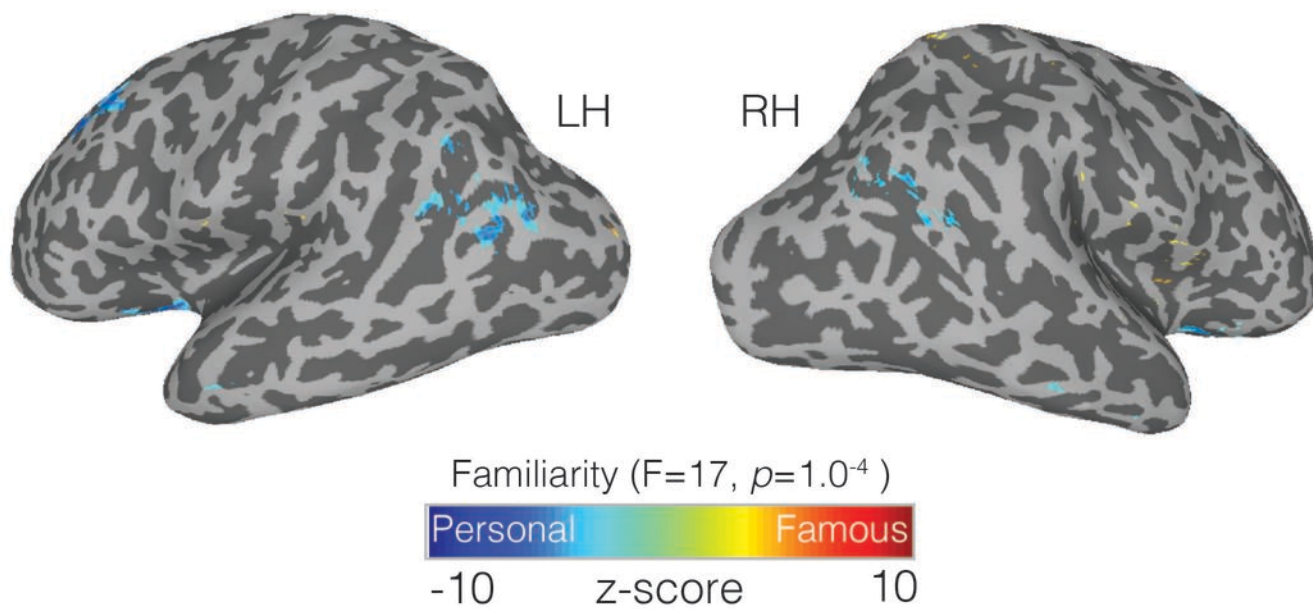
- Personal place peak
- Personal people peak

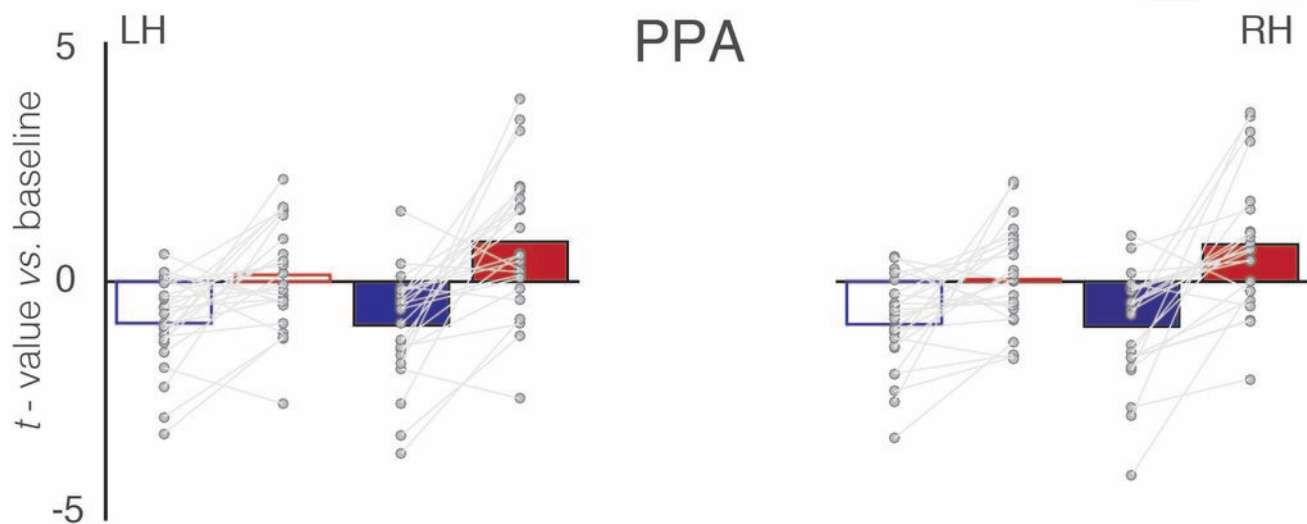


a**b**

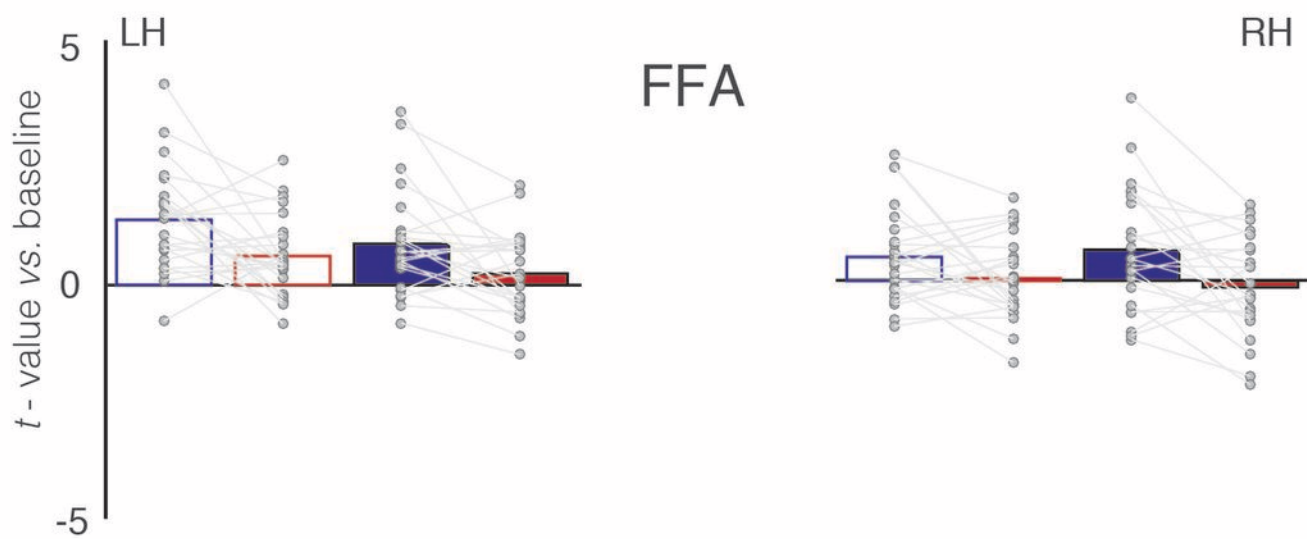




a**b**

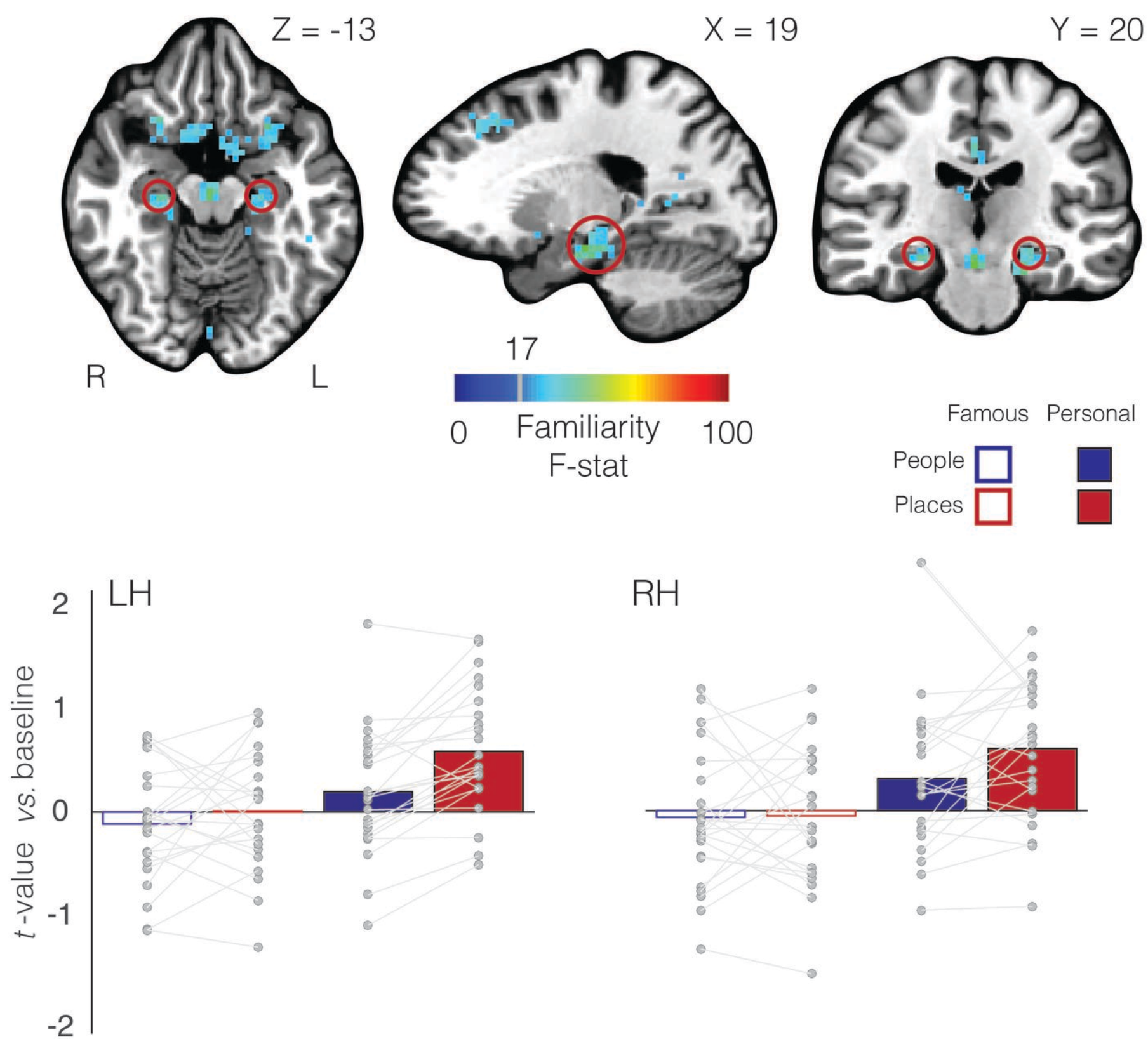


b

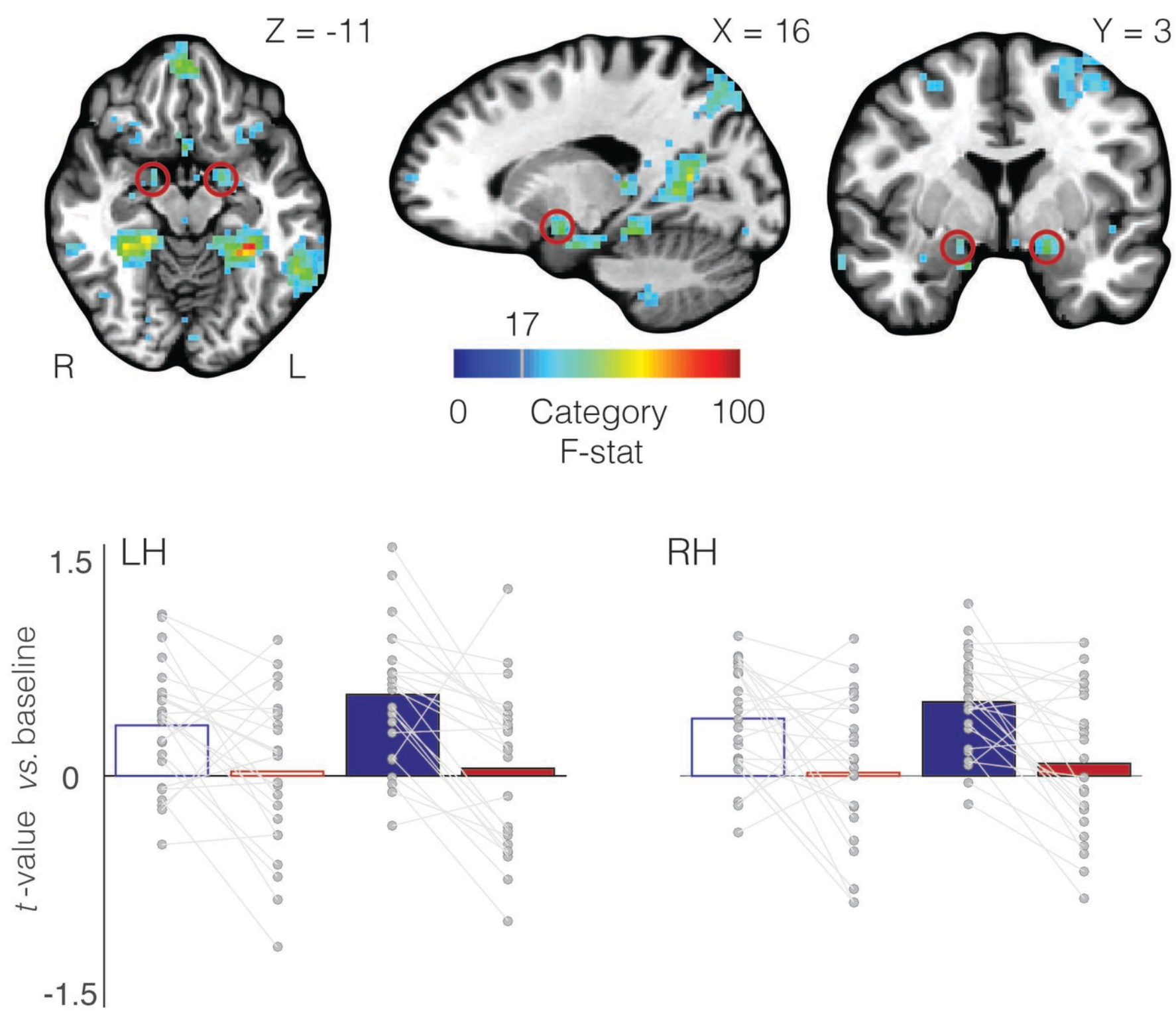


a

Hippocampus

**b**

Amygdala

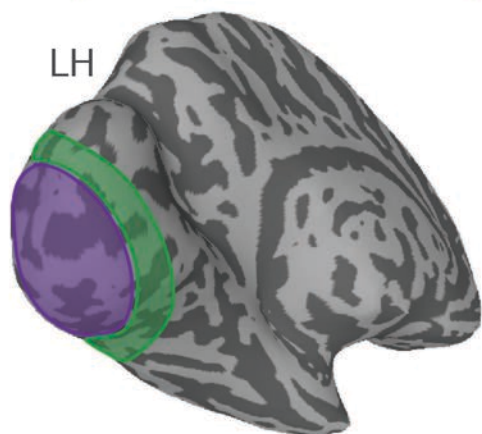
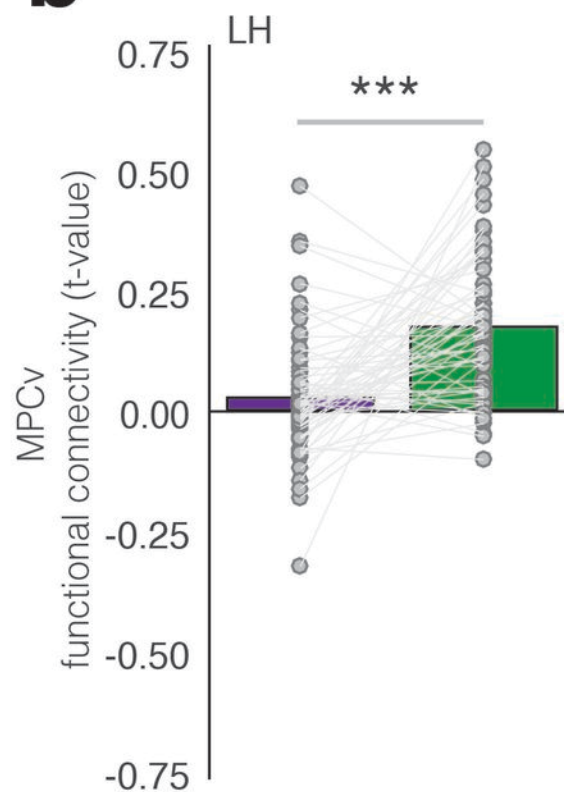


a

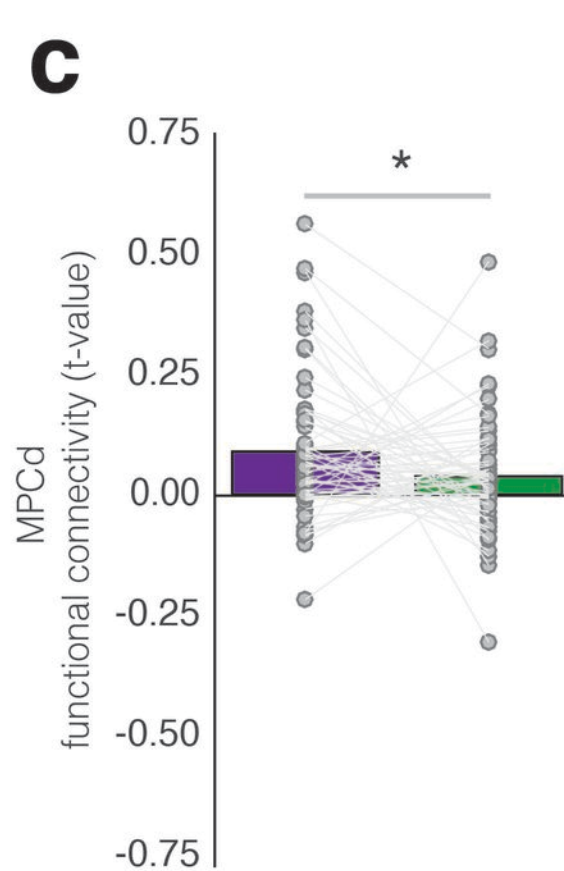
Foveal (0-4° eccentricity)

Peripheral (4-10° eccentricity)

LH

**b**RH

A scatter plot showing functional connectivity (t-value) for MPCv in the RH. The y-axis ranges from -0.75 to 0.75. The plot shows individual data points as gray circles, with a purple box plot for the foveal region and a green box plot for the peripheral region. A horizontal line with three asterisks (***) indicates a significant difference between the two regions.

cns

A scatter plot showing functional connectivity (t-value) for MPCd in the RH. The y-axis ranges from -0.75 to 0.75. The plot shows individual data points as gray circles, with a purple box plot for the foveal region and a green box plot for the peripheral region. A horizontal line with 'ns' indicates no significant difference between the two regions.